INVESTIGATIONS IN FLOW INJECTION ANALYSIS (FIA):

CONVENTIONAL FIA DETERMINATION OF CHLORIDE IN WATER; SEQUENTIAL INJECTION (SI)- FIA DETERMINATION OF MERCURY IN WATER

by

Joanne Cirello-Egamino

A Thesis
submitted to the Department of Chemistry
in partial fulfillment of the requirements
for the degree of
Master of Science

June 1994
Brock University
St. Catharines, Ontario

ABSTRACT

Flow injection analysis (FIA) was applied to the determination of both chloride ion and mercury in water. Conventional FIA was employed for the chloride study. Investigations of the $Fe^{3+}/Hg(SCN)_2/Cl^-$, 450 nm spectrophotometric system for chloride determination led to the discovery of an absorbance in the 250-260 nm region when $Hg(SCN)_2$ and Cl^- are combined in solution, in the absence of iron(III). Employing an in-house FIA system, absorbance observed at 254 nm exhibited a linear relation from essentially 0 - 2000 $\mu g\ ml^{-1}$ injected chloride. This linear range spanning three orders of magnitude is superior to the $Fe^{3+}/Hg(SCN)_2/Cl^-$ system currently employed by laboratories worldwide. The detection limit obtainable with the proposed method was determined to be 0.16 $\mu g\ ml^{-1}$ and the relative standard deviation was determined to be 3.5 % over the concentration range of 0-200 $\mu g\ ml^{-1}$. Other halogen ions were found to interfere with chloride determination at 254 nm whereas cations did not interfere. This system was successfully applied to the determination of chloride ion in laboratory water.

Sequential injection (SI)-FIA was employed for mercury determination in water with the PSA Galahad mercury amalgamation, and Merlin mercury fluorescence detection systems. Initial mercury in air determinations involved injections of mercury saturated air directly into the Galahad

whereas mercury in water determinations involved solution delivery via peristaltic pump to a gas/liquid separator, after reduction by stannous chloride. A series of changes were made to the internal hardware and valving systems of the Galahad mercury preconcentrator. Sequential injection solution delivery replaced the continuous peristaltic pump system and computer control was implemented to control and integrate all aspects of solution delivery, sample preconcentration and signal processing. Detection limits currently obtainable with this system are 0.1 ng ml^{-1} Hg^{o}.

ACKNOWLEDGEMENTS

I would sincerely like to thank Professor Ian Brindle, whose support, encouragement and faith in me will always be remembered. I would also like to thank Shaoguang Zheng for his work on the mercury system and for his many explanations of the flow paths. Thanks are also extended to the members of my committee: Dr. Richardson, Dr. Chiba, Dr. Atkinson, and Dave Boomer; who provided great suggestions and were very encouraging. Thanks to Tim Jones and Donna Vukmanic for their computer and technical support.

I would like to thank Andrea for her friendship, her honesty and her open ear. I would like to thank my family for their support and their love. Finally, I would like to thank my husband Emmanuel, my everlasting source of inspiration and joy, for his love and understanding, now and always.

My experiences at Brock will remain with me always.

TABLE OF CONTENTS

LIST OF TABLES

LIST OF FIGURES

equation to be -1.21 ng mercury. Mercury concentration in laboratory air determined to be 0.014 pg μl^{-1}.

CHAPTER 1: INTRODUCTION

FLOW INJECTION ANALYSIS

(1) HISTORY

Flow injection analysis (FIA) is a technique based on the injection of a liquid sample into a non-segmented, moving carrier stream of reagent. It is a subgroup of the Continuous Flow Analysis (CFA) concept that refers to any process in which the concentration of analyte is measured uninterruptedly in a stream of liquid that travels from point of sample injection to detector. CFA was initially introduced to the scientific community in the early 1950's as a means of automating routine chemical analyses by eliminating the tedious steps of sample and reagent addition and processing for colorimetric or spectrophotometric analysis.[1] The early CFA analyzers consisted of continuous flowing streams, segmented by air bubbles that were initially believed necessary to maintain homogeneity of mixing in large diameter tubinhg and, to prevent sample carryover. It was not until the early 1970's that FIA, continuous flow analysis in the absence of air-segmentation, was introduced as a technique with more power and greater versatility of application than air-segmented CFA. The research groups of Jaromir Ruzicka in Denmark and Kent Stewart in the United States independently examined the effect of injecting the sample directly into the carrier stream and through subsequent studies demonstrated that analysis without air segmentation is both possible and advantageous over CFA, because of its exploitation of

concentration gradients formed by the sample dispersion process.[2,3] Since its introduction in 1975, FIA has become a technique applicable in almost every area of chemical analysis.

(2) PRINCIPLES

Flow injection analysis is based on the combination of three principles: sample injection, controlled dispersion of the injected sample zone, and reproducible timing of its movement from the point of injection to the detector.[4] The simplest flow injection analyzer consists of a pump, to propel the carrier stream through a narrow tube; an injection port through which a well-defined volume of sample solution is reproducibly injected into the carrier stream; and a microreactor in which the sample zone disperses and reacts with the carrier stream, to form a product in sufficient amount to be detected as it is carried through a flow-through detector. Figure 1 illustrates a simple FIA manifold and figure 2 depicts a typical recorder output. The signal generated by the detector has the form of a peak, the height H, area A, or width W of which contains the analytical information. The time span between sample injection and the peak maximum, during which the sample reacts with the carrier stream, is defined as the residence time, T. The sampling cycle of a system is the sum of the residence time T and the baseline to baseline time of the peak, t_b which defines the length of time the analyte spends in the flow-through cell. Typical FIA

Figure 1: A simple single-line FIA manifold ; S is the sample injection port, D is the flow-through cell of the detector, and W is waste. (adapted from reference 5)

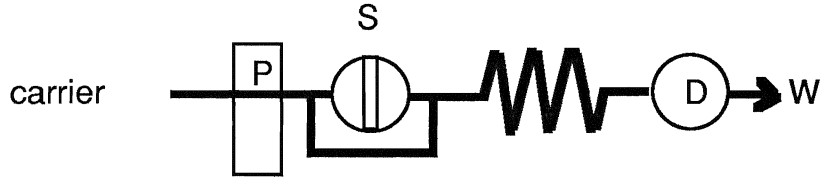

Figure 2: Typical recorder output of an FIA system, S is the time of sample injection, W is the peak width, A the peak area, H the peak height and T the residence time corresponding to peak height measurement. (adapted from reference 5)

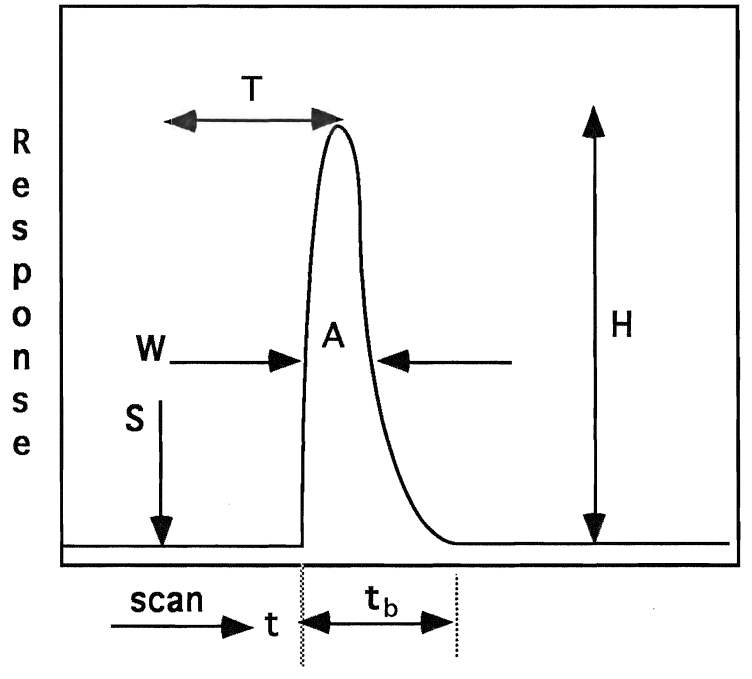

systems have residence times, T, of the order of 5-20 seconds and sampling times of less than 30s. Sample volumes are usually between 1 and 200 µl, requiring reagent volumes on the order of less than 1ml.

The dispersion of a sample within a carrier stream has been defined as the ratio of concentrations of analyte before and after the dispersion process has occurred, in the element of fluid that yields the analytical readout:

$$1. \qquad D = C^{o} / C^{max} = k'H^{o}/k''H^{max}$$

where k' and k'' are proportionality constants. Equation 1 describes the degree to which the sample has been diluted with the carrier stream and encompasses one of the most important principles of FIA. Upon injection of the sample zone, it moves toward the detector while reacting with the carrier stream. The sample zone is dispersed with a parabolic velocity profile, characteristic of laminar flow.[5] In this type of flow, the liquid in the center of the sample zone moves at twice the mean linear speed of the fluid, whereas the layers closer to the outer walls are more retarded. Figure 3 illustrates this phenomenon. Mixing between carrier and sample solution is always incomplete, but because the mixing pattern for a given experimental setup is perfectly reproducible, each subsequent sample is processed in exactly the same way during passage through the channel towards the

Figure 3: Illustration of Parabolic Flow

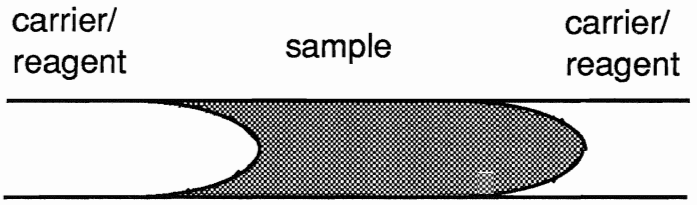

detector. The dispersion of an experimental setup can easily be determined by injection of a specified volume of a colored dye and by the comparison of the peak height with that produced when the flow through cell is filled completely with dye.

Figure 4: Dispersion (D) in an FIA system defined as the ratio between the original concentration C^o and the concentration of the dispersed species, C^{max}. (adapted from reference 5)

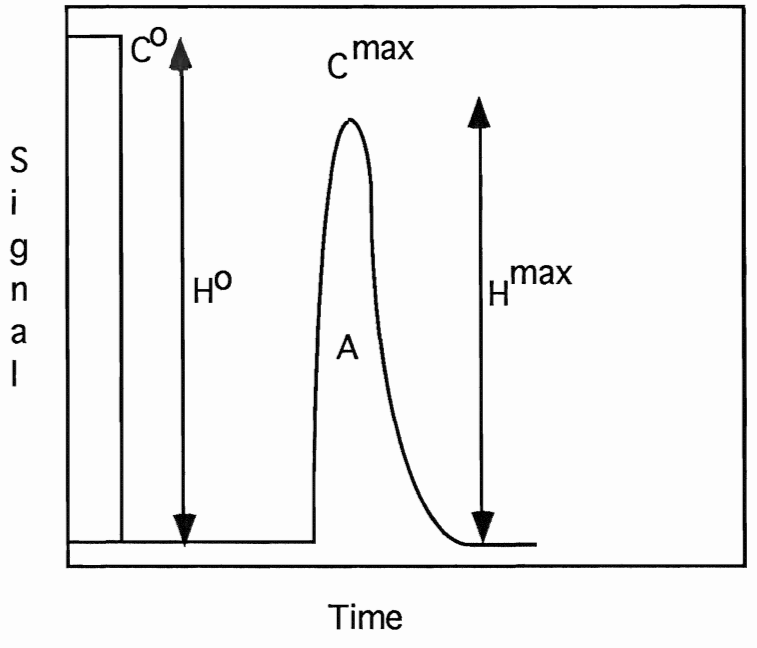

Provided that the Beer-Lambert law is obeyed, k' = k'' and the ratio of the peak heights can be directly related to the dispersion of the system. Figure 4 illustrates important measures used in measuring the dispersion of a system. Dispersion (D) has been classified as limited (D=1 to 3), medium (D=3 to 10) and large (D≥10) and can be manipulated in a system to accommodate the particular analysis.

Several variables have been identified which influence the dispersion of an FIA system. One of the most powerful variables is the sample volume, S_V. If increasing volumes of a dyed solution are injected into an FIA carrier stream, a series of curves will be produced at the detector with increasing peak heights until they reach a steady-state value.

Figure 5 : Response curves as a function of injected sample volume. All curves recorded from the same starting point S with sample volumes of 60,110, 200, 400, and 800 µl. (from reference 5)

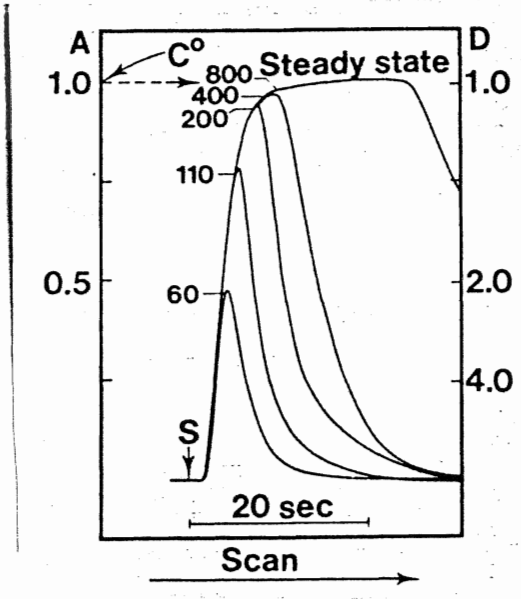

At the steady-state, the absorbance corresponds to the concentration of undiluted dye, and D = 1. Figure 5 illustrates the influence of sample volume. The rising edge of all curves has the same shape regardless of the injected volumes, which can be described mathematically by:

2. $$C^{max}/C^{o} = 1 - \exp(-kS_V) = 1/D \text{ (ref.5)}$$
$$= kS_V$$
(for suitably small values of kS_V)

where k is a proportionality constant and S_V is the sample volume. From equation 2, one can obtain:

3. $$S_{1/2} = 0.693/k$$

where $S_{1/2}$ is the volume of sample solution required to reach fifty percent of the steady-state value, corresponding to D = 2. Figure 5 illustrates that the first portion of the rising curves are linear up to approximately 50% C^{o}, indicating that peak height is directly proportional to injected volume.[5] Equation 2 demonstrates that the dispersion of a system can easily be manipulated by changing the sample volume employed.

In addition to sample volume, the channel length of a system can influence the dispersion and ultimately the peak shape produced at the detector. In a narrow tube of radius r, a specified sample volume S_V occupies a length (l) of the tubing according to the relation:

4. $$l = S_V/\pi\ r^2$$

The same sample volume will occupy increasing lengths of tubing if the diameter is decreased, thus restricting the degree of contact and opportunity for radial mixing between carrier and reagent and lowering the $S_{1/2}$ values. For the purposes of reagent economy, it may be desirable to minimize the diameter of the tubing. However, if the diameters are too narrow, the system may become more complicated as backpressure may require a more sophisticated pump system and filtering of the solutions may be necessary to prevent blocking of the system. It follows from this discussion that the combination of both S_V and channel geometry may allow for manipulation of dispersion of a system. Typically, the optimum internal diameter of tubing connecting the injection port and detector is 0.5 mm for medium dispersion, whereas 0.3 mm is used for limited D and 0.75-1 mm can be used for systems requiring large dispersion[5].

The geometry of the channel connecting the sample injection port and the detector has been shown greatly to influence the dispersion and peak shape of a system. As previously mentioned, the sample zone possesses a parabolic flow profile characteristic of laminar flow. Throughout the 1980's, several researchers attempted to describe mathematically the output curve seen at an FIA detector.[6-10] Their common source of reference was from chemical reactor engineering textbooks that dealt with solution flow in large tubular reactors. The early theory described the peak as predominantly due to the process of axial dispersion of the

sample zone. Further examination of the FIA curves led to the inclusion of the parameter of radial diffusion in order to describe more accurately the curve.

Axial diffusion is defined as diffusion of the elements of fluid in the axial direction, i.e. in the direction of solution flow. Radial diffusion is defined as diffusion from the center of the sample zone towards the outer walls of the reactor tubing. Peak height and shape can be greatly improved if the parabolic velocity profile is disrupted by the promotion of an increased degree of radial mixing. This mixing can be accomplished by creating local turbulence when the direction of flow is suddenly changed. The elements of fluid along the walls of the channel that are lagging are rapidly thrust into the center streamline, whereas those elements initially advancing in the axial direction move closer to the tube walls.[5] The more frequently this process occurs, the greater is the efficiency of mixing between the sample and carrier stream and the more symmetric is the peak shape produced.

In the early days of FIA, the typical channel geometries employed to connect the sample injector and the detector were straight lengths of tubing, coiled lengths of tubing (employed for neatness of appearance), or a length of tubing interrupted by a mixing chamber. With the recognition of the importance of radial mixing to FIA, alternative reactor geometries were designed to promote it. The single-bead string reactor (SBSR), introduced to FIA by Reijn,[11] consists of a length of tubing occupied by beads around which the sample and carrier

solution must pass. In a fashion analogous to mobile phase flow in packed bed chromatography, the path of the stream becomes more tortuous and a high degree of radial mixing occurs. Peaks obtained in the presence of SBSRs are highly symmetrical. Another geometry that promotes radial mixing is the "knitted reactor", initially introduced to FIA by Engelhardt and Klinker.[12] This geometry can easily be created from a straight length of tubing by tightly knotting it. The flow path created in this geometry promotes a very high degree of radial mixing and has proven to be as efficient as the SBSR. Figure 6 illustrates the various channel geometries and their influence on peak shape. The use of a mixing chamber, which was introduced to FIA for titrations, serves clearly to diminish the peak height because the sample zone undergoes significant dilution in the mixing chamber. It is illustrated here for comparison purposes and is almost always avoided in FIA.

Figure 6 : Microreactor geometries commonly employed in FIA: A, straight open tube; B, coiled tube; C, mixing chamber; D, single-bead string reactor (SBSR); and E, knitted reactor.

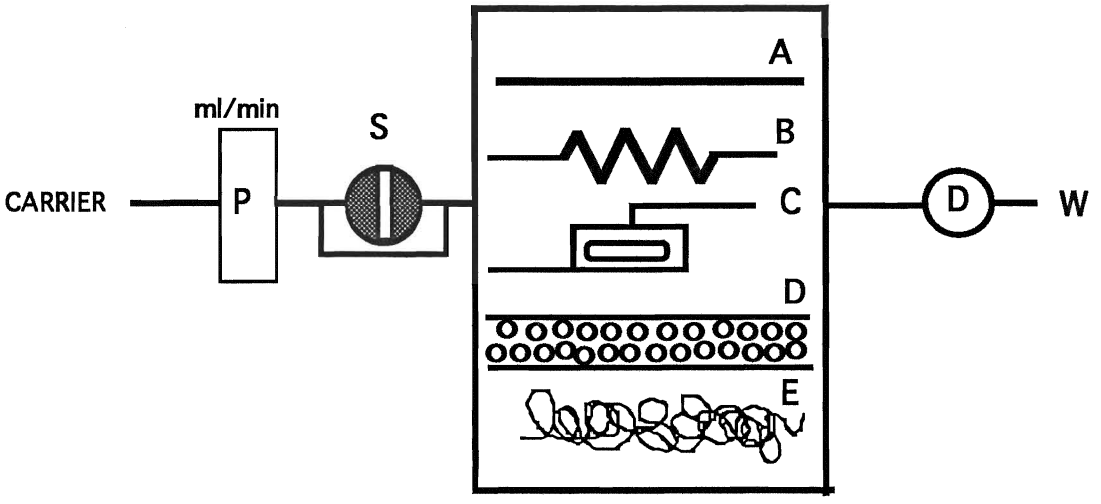

(adapted from reference 5)

(3) MODIFICATIONS/APPLICATIONS OF FIA FOR SPECIFIC TECHNIQUES (SEQUENTIAL INJECTION)

In the early days of FIA, the first procedures adapted to flow systems were colorimetric methods. Simple, one line systems were easily and economically setup to determine analytes such as ammonia, phosphate and glucose[13,14] employing chart recorders to record detector response. Since these early experiments, the complexity of design of FIA systems has increased dramatically to accommodate the growing need for automated, simultaneous multi-component determinations. For example, reactor designs have incorporated solvent extraction to allow for determination of drug metabolites in the pharmaceutical and clinical industries. Karlberg and Thelander[15] extracted caffeine from aqueous acetylsalicylic acid preparations into chloroform and by separating the aqueous and organic streams, were able to divert the aqueous phase to waste while transporting the organic phase to the flow-through cell of a spectrophotometer. Gas diffusion was coupled with FIA systems by incorporating a gas-permeable membrane in the reactor design that served to separate the sample stream and the gas colour reagent stream. Total CO_2 in blood plasma was measured by Baadenhuijsen and Seuren-Jacobs[16] in 1979 employing this method. Packed reactors have also been incorporated into FIA systems to catalyse, provide reagent, or preconcentrate analyte. For example, Almuiabed and Townshend[17] utilized solid $Hg(SCN)_2$ packed columns instead of an aqueous $Hg(SCN)_2$ reagent stream

for chloride ion determination. Enzymes or antibodies have been immobilized on inert beads to facilitate kinetic studies of catalysis or antigen binding.[18,19] The current number of methodologies present in the FIA field is quite large and rapidly increasing. It is beyond the scope of this thesis to present them all here, but a complete compilation of FIA applications and references may be found in reference 5 (second edition).

The exploitation of the concentration gradients formed by the dispersion process of the flowing stream allowed for the evolution to a new class of FIA methodologies. Techniques developed by the manipulation of flow properties include stopped-flow and sequential injection flow systems.[5] Stopped-flow measurements are performed by stopping the carrier flow when the mixture of sample plug and reagent reaches the detector. Dispersion of the sample zone halts in the absence of flow and reaction rate measurements are possible if the sample zone is trapped in the flow cell. Stopped-flow techniques have been successfully employed for kinetic measurements of biologically active compounds.[20] The sequential injection flow technique[21] employs a selector valve rather than an injection valve to transport sample and reagent solutions into a holding coil (figure7). Sinusoidal flow, rather than linear flow is generated by a cam driven sinusoidal pump, which permits the load and measurement cycle to occur within a single revolution of the circular cam (figures 8,9). The integration of a sinusoidal flow pump with

an electronically actuated multiport selector valve allows synchronized sample zone injection and stream switching. During the load cycle, a stack of well-defined zones is produced in the holding coil, which is then

Figure 7: Diagram of a sequential injection system, consisting of a piston pump, holding coil, reaction coil, an eight-port selector valve, and a detector. (Bottom) Schematic diagram of sequenced zone structure and zone interpenetration.

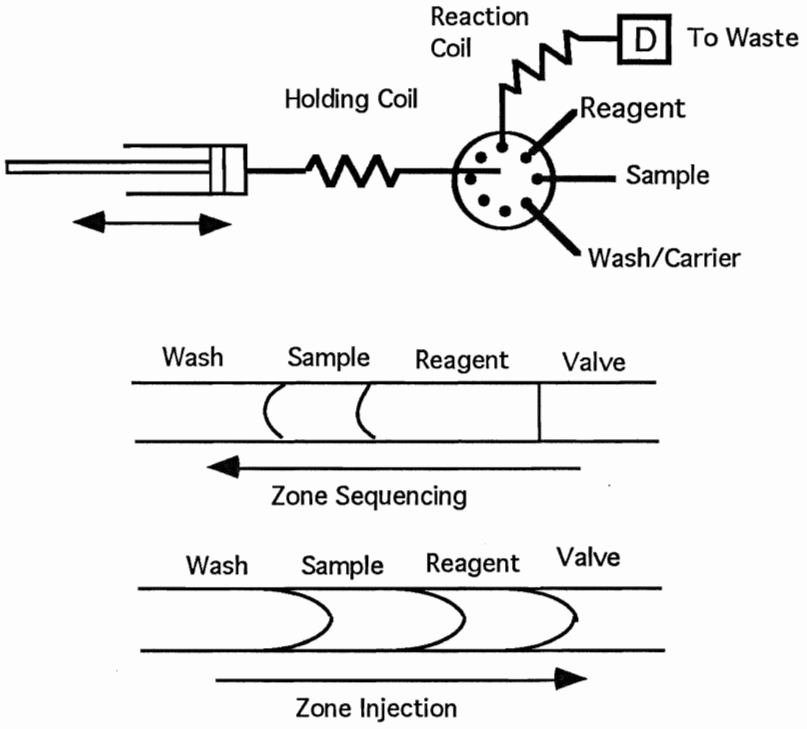

(adapted from ref.20)

Figure 8: Representation of sinusoidal flow pump. (adapted from reference 21).

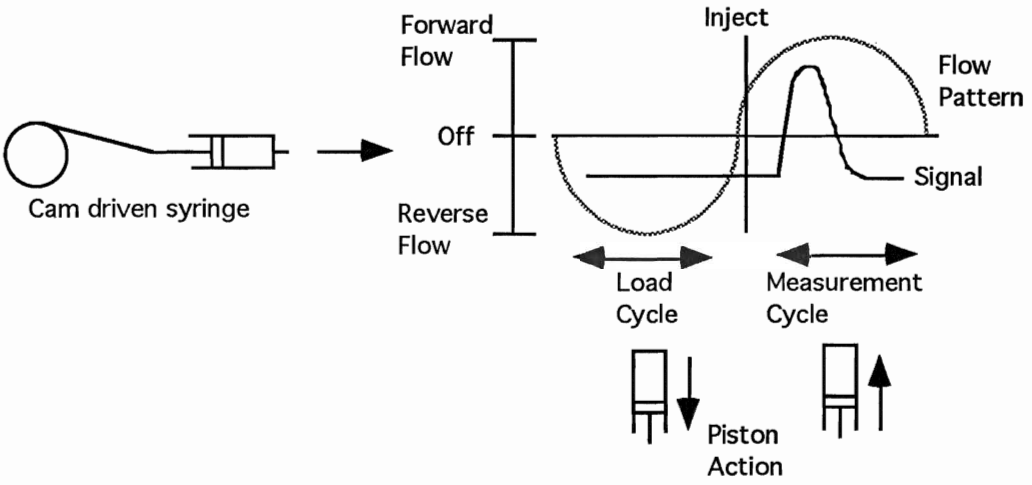

Figure 9: Flow-injection manifold employed with the sinusoidal flow pump and the eight-port valve.[21] A represents load cycle, B represents measurement cycle.

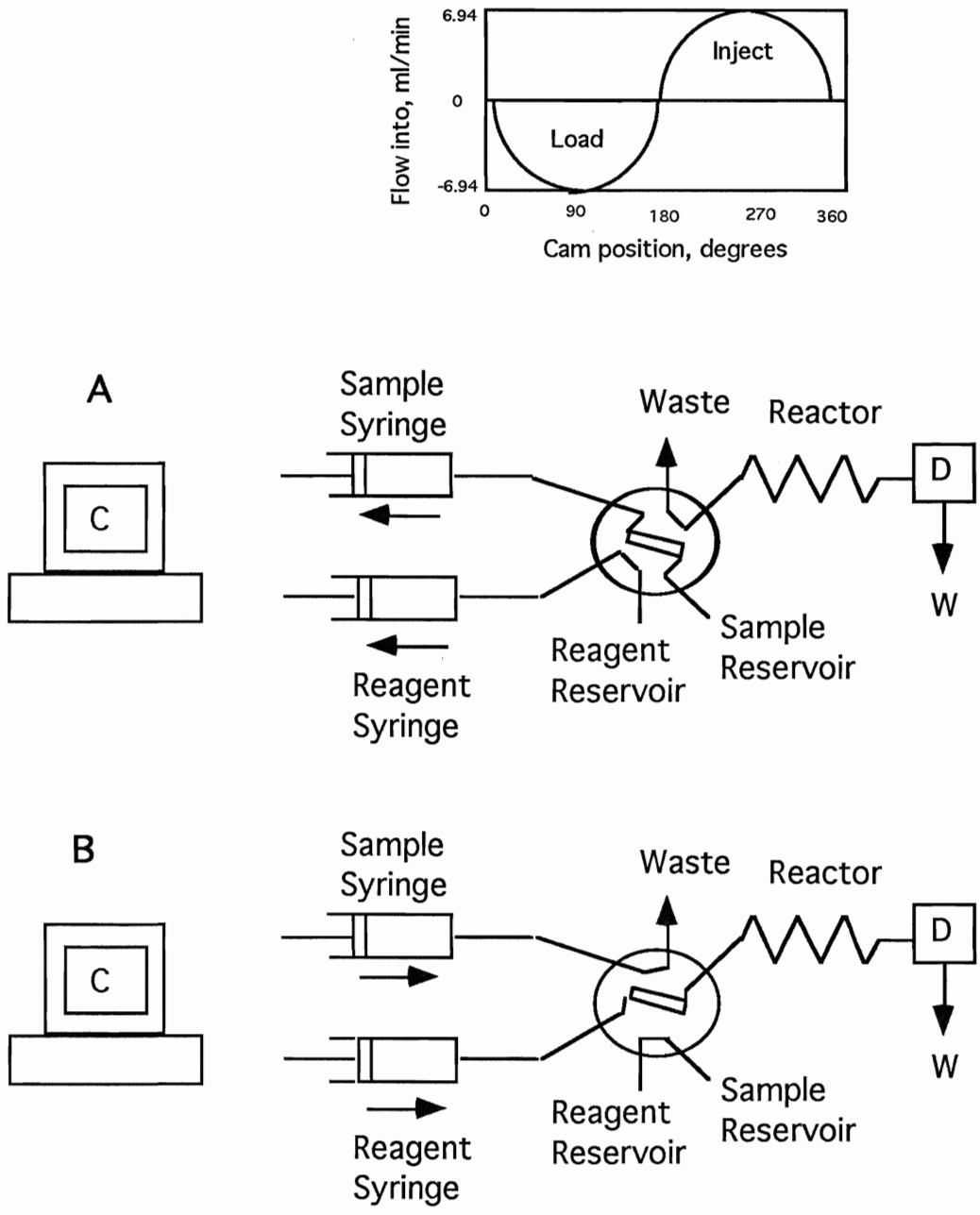

injected towards the detector by flow reversal. The advantages of sequential injection over the conventional continuous flow techniques include: (1) only a single valve and pump are employed in SIA, regardless of the number of solutions, (2) solution volumes are determined by piston stroke length, not channel lengths, simplifying the design and tubing requirements of the system, (3) the degree of dispersion can be finely controlled by the length and number of flow reversals, (4) the reaction time can be adjusted by the inclusion of stopped-flow periods.[22] The primary difference between SI and conventional FIA occurs in the number of sample/reagent interfaces that occur in the line. In FIA the sample zone is surrounded on either side by reagent, as illustrated in figure 3, creating two reaction zones separated by unreacted sample. As a result, double peaks can be observed in FIA systems. Zone sequencing in SI systems ensures that double peaks do not occur. Only one interface between sample and reagent is present (figure7), as the carrier solution is different from the reagent.

CHLORIDE DETERMINATION

(1) IMPORTANCE OF STUDY

Chloride ion is widely distributed in nature, being present in surface, ground and domestic waters in varying concentrations. The chloride content in freshwater is typically below 120 $\mu g\ ml^{-1}$, but in surface and domestic water the concentration of chloride ion may reach levels

greater than 1000 μg ml^{-1}. The determination of chloride ion is important in both the clinical and environmental areas of analytical chemistry. Determinations of chloride ion are performed daily at water treatment plants to monitor the quality of tap water. Power plants require rapid chloride monitoring methods to prevent accumulation of Cl^-, resulting in corrosion of metal components of steam-generating systems. In clinical analyses, the determination of chloride in blood serum samples is a routine test performed daily in medical laboratories.

(2) UTSUMI'S METHOD: MODIFICATIONS AND DRAWBACKS

Many analytical methods for chloride determination were developed in the early to mid 1900's. The gravimetric method, involving the precipitation of chloride ion as silver chloride, and the volumetric Volhard and Mohr methods[23-26] comprise what are currently defined as the classical methods of chloride determination. Because these methods lack the sensitivity required for the analysis of Cl^- concentrations below 50 μg ml^{-1}, spectrophotometric methods were developed to determine chloride at these levels. The mercurometric method, developed in 1933 by Dubsky and Trtilek,[27] employs diphenylcarbohydrazide as the indicator in the titration with mercuric nitrate. Problems of reproducibility due to the large number of variables of this system make it impractical for routine chloride determinations.

In 1952, Utsumi *et al.*[28,29] introduced the mercury thiocyanate spectrophotometric method for chloride determination. This method employs $Hg(SCN)_2$ and Fe^{3+} as reagents and is based on the displacement of thiocyanate ion from mercury thiocyanate by chloride and subsequent reaction of the liberated thiocyanate with iron(III), to form a reddish-orange iron(III)-thiocyanate complex, detectable at 450 nm. The sequence of reactions involved in the formation of $Fe(SCN)^{2+}$, that have been proposed, are:

5. $Hg(SCN)_2 + 2Cl^- \Leftrightarrow HgCl_2 + 2SCN^-$
6. $SCN^- + Fe^{3+} \Leftrightarrow Fe(SCN)^{2+}$ (red, 450nm)

The linear analytical range of Utsumi's method is 0.1 - 20 μg ml^{-1} Cl^- in water.[37] This method is currently employed for the determination of chloride ion in clinical and industrial laboratories worldwide.[30-33] Skeggs and Hochstrasser[34] developed an automated method for analysis of blood serum that included the mercury thiocyanate/iron(III) determination of chloride ion in 1964. A commercial chloride autoanalyzer, based on the work of Skeggs and Hochstrasser was introduced by Technicon Corp.[35] in 1974. Modifications of the working conditions have been implemented by various researchers over the years in order to improve the linearity and sensitivity of this detection method, mainly through the incorporation of sample dilution components into the flow system. For example, Ruzicka and Stewart[36] introduced stream sample

splitting into their chloride determination flow manifold as a means of expanding the reported[37] analytical range from 0.1-20 μg ml^{-1} up to 100 μg ml^{-1} chloride ion without loss of reproducibility. Stream sample splitting was also employed by Basson and van Staden[38] as a means of both diluting and facilitating simultaneous determination of chloride and sulphate ion in solution. They were able to extend the analytical range up to 300 μg ml^{-1} chloride. In 1985, van Staden[39] proposed pretreatment of samples using an automated prevalve dilution technique. Chloride samples of 0-800 μg ml^{-1} were analyzed with this method. Recently, van Staden[40-42] has employed dialysis to allow for both dilution of sample and separation of several detectable species. Modifications resulting in improvements of the detection limit were introduced by Tyson *et al.*[43] in 1989. A double-line manifold, pulse dampers, a packed bed reactor, and a delay coil were employed to eliminate baseline problems associated with refractive index changes, reagent absorption and valve switching peaks. Tyson was able to obtain a linear range from the detection limit of 4.5-8.0 $x10^{-3}$ μg ml^{-1} to 2.00 μg ml^{-1} Cl^-. The linear analytical range obtainable with the iron(III)/$Hg(SCN)_2$/Cl^- system has posed a serious limitation on the employment of this method to determination of aqueous samples containing chloride concentrations above 100 μg ml^{-1}.

In the decades since the original research by Utsumi, little insight has been gained on the interactions that occur

between iron(III), $Hg(SCN)_2$ and Cl^-. Early papers[44] reveal that the focus of interest in this reaction was on confirming and establishing the identity of the reaction product, $Fe(SCN)^{2+}$. Little work has been published on the identification of intermediate complexes formed to confirm the accepted mechanism of this reaction. The dissociation and formation constants for the individual reactions are:

7. $Hg(SCN)_2 \Leftrightarrow Hg^{2+} + 2SCN^-$

$K_d(Hg(SCN)_2) = 3.3 \times 10^{-18}$

8. $HgCl_2 \Leftrightarrow Hg^{2+} + 2Cl^-$

$K_d(HgCl_2) = 6.06 \times 10^{-14}$

9. $Fe(SCN)^{2+} \Leftrightarrow Fe^{3+} + SCN^-$

$K_f(Fe(SCN)^{2+}) = 126$

(values from ref. 45)

Consideration of the dissociation constants above suggests that this series of reactions should not proceed to the extent that they do because of the large difference in the K_d values for $Hg(SCN)_2$ and $HgCl_2$. Commenting upon the unlikeliness of the reaction, Florence[46] observed that " . . . this remarkably useful reaction is at best only just thermodynamically possible". If the formation constants of the individual reactions are employed, the overall equilibrium constant for Utsumi's system (equation 10) can be calculated:

10. $Hg(SCN)_2 + 2Fe^{3+} + 2Cl^- \Leftrightarrow HgCl_2 + 2Fe(SCN)^{2+}$

where $Keq = \frac{K_f(HgCl_2)}{K_f(Hg(SCN)_2)} \cdot K_f(Fe(SCN)^{2+})^2 = 0.5$

Initial research in our laboratory examined the $Fe^{3+}/Hg(SCN)_2/Cl^-$ system, in an attempt to understand why the process occurs. One of the experiments performed revealed that, when $Hg(SCN)_2$ and Cl^- ion are combined in the absence of iron(III), an absorption at 254 nm is observed that rises proportionately with chloride concentration. The focus of the study was shifted to the examination of the interactions between $Hg(SCN)^2$ and Cl^- in water. This thesis reports investigations into the application of the reaction between mercury thiocyanate and chloride for the determination of chloride in water, employing FIA.

MERCURY DETERMINATION

(1) IMPORTANCE OF STUDY

Exposure to mercury and its species continues to pose a threat to all life forms. Although the toxicity of mercury and mercury salts has been known for centuries, widespread concern on regulating levels in the environment did not appear until worldwide knowledge of the Minimata Bay mercury poisoning epidemic in Japan in the 1950's.

Mercury, in any form, is not essential to man for any biological or physiological process. Elemental mercury is readily absorbed into the body through the skin or by inhalation of its vapour. The species of mercury commonly found in the environment include elemental mercury, inorganic mercury salts such as $HgCl_2$ and Hg_2Cl_2, organic monoalkyl halide salts such as CH_3Hg^+, dialkyl compounds and organic compounds such as diphenyl mercury.[47]

Mercury vapour is readily absorbed through inhalation, the gastrointestinal tract and unbroken skin. The effects of mercury poisoning are cumulative due to the fact that it passes very slowly through the body. Prolonged exposure to mercury vapour results in permanent damage to the nervous system, although the toxic effects may go unnoticed until extensive damage has already occurred.

Victims of inorganic Hg poisoning experience symptoms including nausea, abdominal pain and diarrhea, followed by gingivitis, digital tremors hallucinations, and ultimately death due to extreme exhaustion. Monoalkyl salts and dialkyl

mercury compounds cause the most severe and debilitating symptoms. They affect the central nervous system and cause focal cerebral and cerebellar atrophy, leading to vision loss.

The level of mercury in the environment has increased during this century as a result of technological advances in industry, agriculture and medicine. Mercury is found in thermometers, barometers and diffusion pumps in scientific laboratories. It is employed in the production of pesticides, chlorine, batteries and was commonly employed in dentistry. The disposal of industrial mercury wastes into rivers and oceans results in accumulation of mercury in sediments. Fish trap and store methylmercury salts and dimethylmercury in their tissues and fat deposits, introducing these toxins into the food chain.

The Minimata epidemic that occurred in Japan was caused by people eating methylmercury contaminated fish. The contamination was linked to the industrial wastes of vinyl chloride-acetic acid factories that dumped methylmercury containing effluent into the bay. The plant used mercuric sulfate as a catalyst to convert acetaldehyde to vinyl chloride and the inorganic mercury had been partially methylated in the plant. The disastrous effects of the Minimata[48] tragedy revealed the necessity of monitoring and regulating the level of mercury in the environment.

(2) REVIEW OF METHODS

The heightened awareness of mercury toxicity in the scientific community led to extensive research and the development of techniques for mercury determination in a vast variety of samples. The current, most extensively employed method for mercury determination is cold-vapour atomic absorption spectrometry (CV-AAS) introduced by Hatch and Ott[49] in 1968. Employing this method, aqueous inorganic mercury is reduced to volatile elemental mercury by a reducing agent such as stannous chloride or sodium borohydride. Atomic mercury is stripped from solution into the gas phase and is transported to the quartz cell for detection via atomic absorption. Equation 11 represents the reduction process.

11. $$Sn^{2+} + Hg^{2+} \Leftrightarrow Sn^{4+} + Hg^{o}$$

The system, as developed by Hatch and Ott, experienced poor detection limits, due to the use of a large reaction vessel and, in addition, because the partition coefficient of mercury between the solution and gas phase favours solution.[50] Modifications to the system were made by several researchers[51,52] to improve the efficiency of diffusion of mercury into the carrier gas, minimize the dead volume of the system and increase the efficiency of transport of the Hg plug to the absorption cell. For example, Gilbert and Hume[51] incorporated a porous frit into the reduction vessel, which resulted in greater efficiency of Hg diffusion into the gas

phase. Hawley and Ingle[53] miniaturized this system and, by minimizing the sample volume and carrier gas volume, they were able to increase the sensitivity of mercury detection dramatically. They were able to reduce the detection limit of the system to 1 pg ml^{-1} from the 1 ng ml^{-1} value, obtained by Hatch and Ott. These researchers also dealt with the problem of mercury losses from sample solutions and proposed the use of oxidizing agents and acid as preservatives. Other improvements on the mercury detection system included the incorporation of automated sample and reagent delivery. Oda and Ingle[54] employed a peristaltic pump to deliver sample and reagent to the reduction vessel which resulted in more rapid sample analysis.

The detection of aerated mercury by atomic fluorescence was investigated by Thompson and Godden[55] in 1975. AAS detection of Hg presents several disadvantages to researchers, including non-linear responses and difficulty in measurement of low Hg levels. Atomic fluorescence is ideal for Hg determination as mercury is atomic at room temperature and absorbs and fluoresces at the same wavelength. Early systems employing AFS detection were modified AAS instruments but an instrument designed specifically for Hg determination via AFS was introduced by Godden and Stockwell[56] in 1989. Detection limits below 0.02 ng ml^{-1} were reported using their system. The main advantages over the CVAAS systems are : simplicity of design and construction, inexpensive, and high sensitivity. This system was recently integrated with flow

injection analysis by Corns *et al.*[57] who revealed the effects of injecting small sample sizes on the minimization of carryover. A commercial mercury analysis system, developed through the joint efforts of C. Vandecasteele's and R. Dams' research group in Belgium and R. Dumarey's group[58] is currently available from P.S. Analytical in the U.K.

(3) PS ANALYTICAL'S MERCURY DETERMINATION SYSTEM

The PSA 10.511 mercury determination system obtained (figure 10), consists of the GALAHAD mercury concentration system that incorporates a set of switching valves and a gold amalgamator that acts to preconcentrate elemental mercury in a series of steps before sending it to an accompanying fluorescence detector. The use of amalgamation onto gold is based on the affinity of mercury for the noble metals and has been employed by several researchers as a means of preconcentrating mercury.[59-64] In order for this system to be employed successfully, all forms of mercury to be determined must be converted to inorganic mercury, which can then react with a reducing agent (i.e. $SnCl_2$) that converts it to elemental Hg that is stripped from solution and transported over the gold trap for amalgamation. The fluorescence detector is the PSA MERLIN which generates signals, that can be recorded as peaks by a chart recorder, for incoming mercury samples. The system allows for mercury determination in air through syringe injection or for aqueous sample analysis via the incorporation of a gas liquid separator. The mode of operation

of this system is described in more detail in the instrumental section.

Figure 10: PSA 10.511 Galahad/Merlin Mercury Determination system.

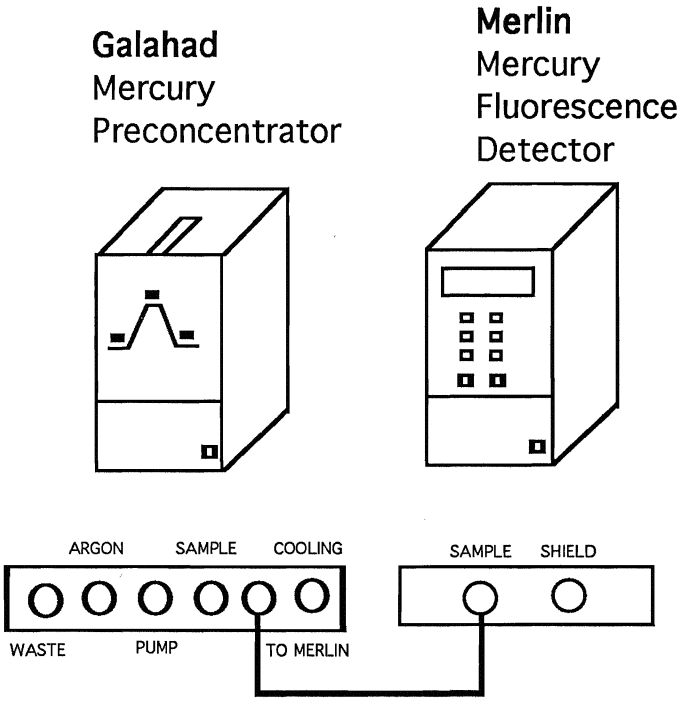

CHAPTER 2: EXPERIMENTAL

REAGENTS

(a) CHLORIDE DETERMINATION

All chemicals employed were of analytical reagent grade. A saturated mercury thiocyanate solution (0.070% m/v, 2.2 x10^{-3}M) was prepared by stirring 1.0 g of $Hg(SCN)_2$ (Aldrich) in distilled water overnight. The saturated solution was filtered into a clean flask and was used as a stock solution from which dilutions were prepared as needed. Chloride ion solutions were prepared by dilutions of appropriate amounts of stock NaCl (BDH), 1000 μg ml^{-1} solution in distilled water. A 0.1M Fe^{3+} solution in 0.1M HNO_3 was prepared by adding 4.04 g $Fe(NO_3)_3 \cdot 9H_2O$ (BDH) to a 100 ml volumetric flask containing 10 ml 1M HNO_3 and diluting to the mark with distilled water. A 0.01 M KSCN solution was prepared by adding 0.10 g of KSCN (BDH) to a 100 ml volumetric flask and diluting to the mark with distilled water. Solutions of 1000 μg ml^{-1} Br^-, I^-, SO_4^{2-}, Ca^{2+}, and Mg^{2+} were prepared by dissolving the appropriate amounts of analytical reagent grade KBr (BDH), NaI (BDH), K_2SO_4 (Fisher), $Ca(NO_3)_2 \cdot 4H_2O$ (BDH) and $Mg(NO_3)_2 \cdot 6H_2O$ (BDH), respectively, with distilled water. A 0.1M HNO_3 solution was prepared from concentrated HNO_3 (BDH) which was used to rinse all glassware and tubing of the FIA setup. Standard addition solutions for FIA analysis were prepared by adding 20.00 ml of laboratory tapwater to various volumes of 1000 μg ml^{-1} Cl^-. The pH was adjusted to 1 with concentrated nitric acid to eliminate dissolved carbonate and

sulphide, and the solutions were diluted to 100 ml with distilled water. Increments of 0, 50, 100, 150, and 200 μg ml^{-1} of Cl^- were added to solutions for the FIA standard addition determination. Standard addition solutions for UV analysis were prepared by pipetting specific volumes of tapwater, $Hg(SCN)_2$, Fe^{3+}, and Cl^- into 10 ml volumetric flasks, adjusting the pH to 1 with HNO_3 and diluting to volume with distilled water. Samples containing 0, 10, 30, 50 and 70 μg ml^{-1} added Cl^- were prepared for study at 450 nm. Solutions for interference studies were prepared by combining appropriate volumes of the interference ion solutions with 10.00 ml of 1000 μg ml^{-1} Cl^-. The pH of the solutions were adjusted to 1 with HNO_3 and were diluted to the mark in 100 ml volumetric flasks with distilled water. Solutions containing interferents at levels from 0 to 100 μg ml^{-1} were prepared and tested.

(b) MERCURY DETERMINATION REAGENTS

All reagents employed were of analytical reagent grade. A stock 1000 ppm mercuric chloride solution was prepared by adding the appropriate amount of $HgCl_2$ (BDH) to 5.0 ml concentrated nitric acid (Merck, 0.0000005% max Hg) in a 100 ml volumetric flask and diluting to volume with distilled H_2O. This solution was stored at 4 C and dilutions were prepared as needed. A 5% m/v stannous chloride reducing solution was prepared by adding 5.0 g $SnCl_2 \cdot 2H_2O$ (BDH) to 7.0 ml concentrated HCl (BDH) and 1 piece of tin metal (Fisher

Scientific) to avoid oxidation of $SnCl_2$. The solution was diluted to the mark in a 100 ml volumetric flask with distilled water. Nitric acid (1M), prepared from concentrated acid, was employed for the wash and carrier solutions. All glassware was washed and soaked in dilute HNO_3.

For the mercury in air studies, elemental mercury was placed into a vial with a septum lid. The vial was then transferred into a water bath. The temperature of the mercury vapour was monitored for calculation of the saturation concentration of atomic mercury in air via the equation[65]:

$$12. \quad C = \frac{3216522.61}{T} \times 10^{-(A+B/T)} \qquad *$$

Where : C is Mercury concentration in air (ng ml-1)
A = -8.1334459741
B = 3240.871534
T = Absolute temperature in Kelvin

(* The number of significant figures employed by Weast and by PS Analytical is surely questionable. The following version was employed in this work:)

$$C = \frac{321.7 \times 10^4}{T} \times 10^{-(A + B/T)}$$

with: A = -8.133
B = 3.241×10^3
T = absolute T in Kelvin (to 4 sig.figs.)

Injections of mercury saturated air were made via syringes (Hamilton Co., Reno, Nevada) through the syringe injection port of the PSA Galahad.

APPARATUS

(1) CHLORIDE DETERMINATION

UV studies were performed on a Varian DMS 100 UV-visible spectrophotometer (Varian Instrument Group, Sunnyvale, California, U.S.A). Initial flow injection work was performed on a Perkin Elmer Series 3 high performance liquid chromatograph with a UV detector, equipped with a digital scanner (Perkin Elmer, Minnesota, U.S.A). A Gilson Minipuls 3 peristaltic pump (Gilson, Ohio, U.S.A.) was used to deliver sample solution to the 20 µl sample loop of the Rheodyne Type 7000 (Rheodyne Inc., California, U.S.A) valve, while the HPLC pump simultaneously propelled $Hg(SCN)_2$ solution (0.012%) to the detector. Manual switching of the valve introduced the sample into the flowline towards the detector. Figure 11 illustrates the flow manifold.

Figure 11: Flow manifold of initial FIA setup utilizing Perkin Elmer instrument.

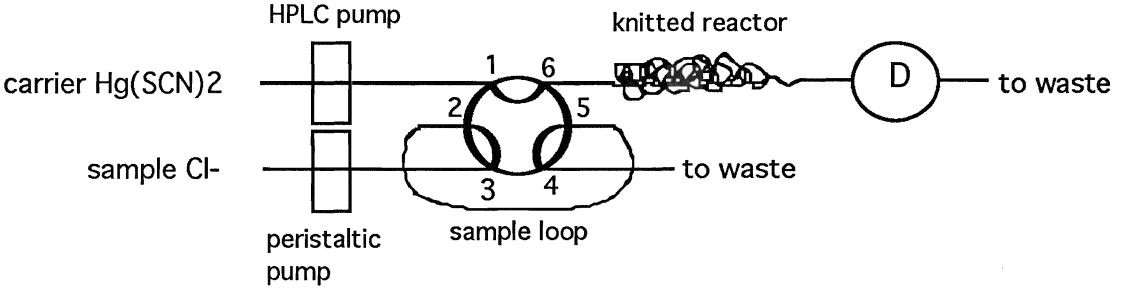

An in-house FIA system was created using the optical path of a Unicam SP90 AA Spectrophotometer with a mercury

hollow cathode lamp (Perkin Elmer) as the 254 nm optical source. The Gilson peristaltic pump delivered both the carrier, mercury thiocyanate solution, and the chloride sample to the Rheodyne valve. Switching of the valve from the load to the inject position introduced the sample plug (2.5-20 µl sample loops employed) into the mainstream flow, through a length of knotted tubing, and thence to the detector. Detection was achieved as the solution passed through a 1mm x 10mm Hellma type 178.313, 8 µl flow-through cell (Hellma, Concord, Ontario, Canada) which was positioned in the optical path of the spectrophotometer. Peristaltic pump tubing was employed to propel the carrier and sample solutions throughout the system and tygon tubing (0.5 mm i.d.) connected the sample introduction point of the line to the flow-through cell and was used for the knitted reactor. Figure 12 illustrates this flow manifold.

Figure 12: Flow manifold of in-house FIA system.

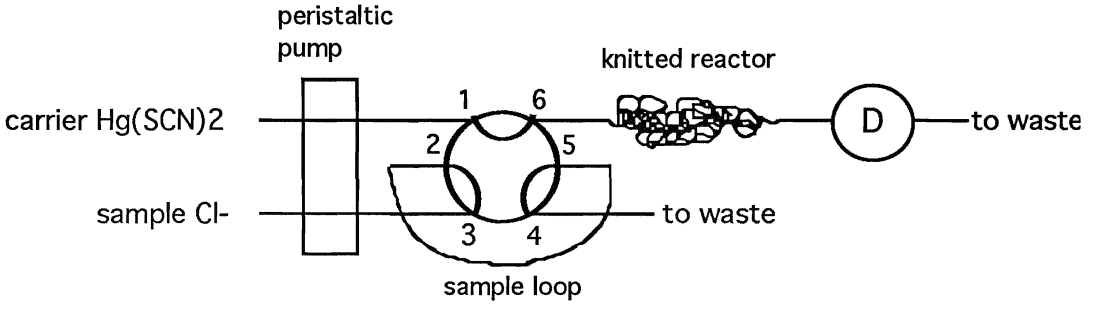

(2) MERCURY DETERMINATION INSTRUMENTATION

Description of PSA 10.511 Galahad/Merlin System

The GALAHAD mercury concentration system incorporates a set of switching valves and a gold amalgamator that concentrates elemental mercury in a series of steps before sending it to the MERLIN fluorescence detector. The detector generates signals that can be recorded as peaks by a chart recorder. The gold amalgamator/heating assembly of the PSA Galahad is illustrated in figure 13.

Figure 13: Heating assembly of PSA Galahad. (adapted from reference 66)

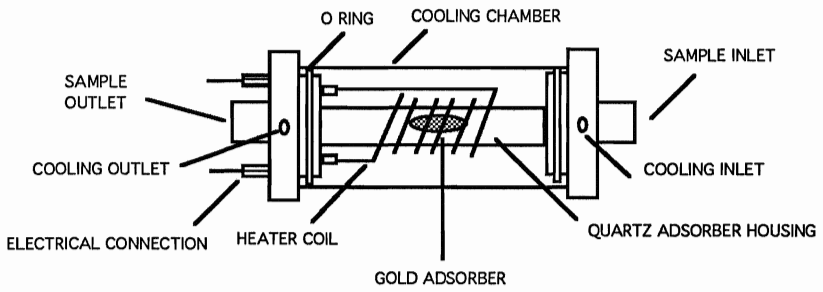

The quartz tubing surrounding the gold mesh is covered by a coil of nichrome wire that is connected to a power supply, which heats the coil to 450 C to revaporize amalgamated Hg^0. The quartz tube and wire assembly are housed within a cooling chamber which permits a cooling gas to pass rapidly over the coil to cool the wire and amalgamator.

Figures 14 (A), (B), (C), and (D) illustrate the original flow schematics for the GALAHAD system. The valve directs the gas flow over the gold trap. During the Amalgamation Stage, which is also the default configuration of the valving

system, the valve settings allow for air or gas flow to continually pass over the gold trap. Once the GALAHAD system is manually activated, the valves change to the Flush configuration, during which air is flushed out of the system by argon carrier gas. This stage is followed by the Vaporize stage, during which the nichrome wire surrounding the quartz tube of the gold trap is resistively heated to 450 C. This results in the release of adsorbed mercury from the gold trap and its transport to the detector, which generates the signal.

The final stage is the Cool stage, during which the heater coil and the gold trap are cooled to prepare for the next amalgamation cycle. At the onset of the cool cycle, the valving configuration changes to the same as the Amalgamation configuration, preparing the system for the next sample analysis (refer to figures 14 (A), (B), (C), and (D) for valve configuration).

The series of Flush, Vaporize and Cool stages collectively comprise the Hg Determination cycle of the Galahad system. The foregoing discussion describes the operation of the GALAHAD/MERLIN system as received from PSA Analytical.

Mercury determination in aqueous samples involved a gas/liquid separator (in-house construction) for aeration of Hg^0 from solution. A Gilson Minipuls 3 peristaltic pump (Gilson, Ohio, U.S.A.) was employed to deliver reagent and wash solutions to the separator and sample to the 50 µl sample loop

of a switching valve, the manual switching of which injected the sample into the carrier stream to the gas/liquid separator.

Figure 14 : Valving configurations of the PSA Galahad: A, Amalgamation ; B, Flush ; C, Vaporize; D, Cool.

Mercury Amalgamation

(A) AMALGAMATION

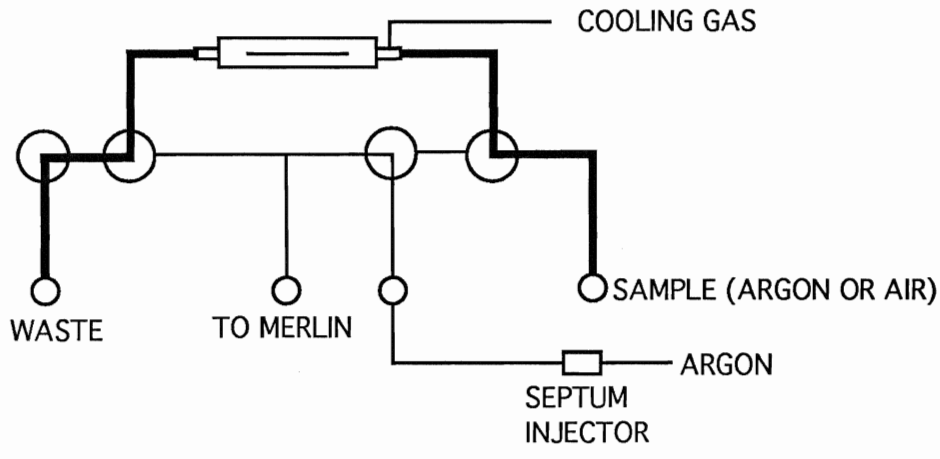

Mercury Determination

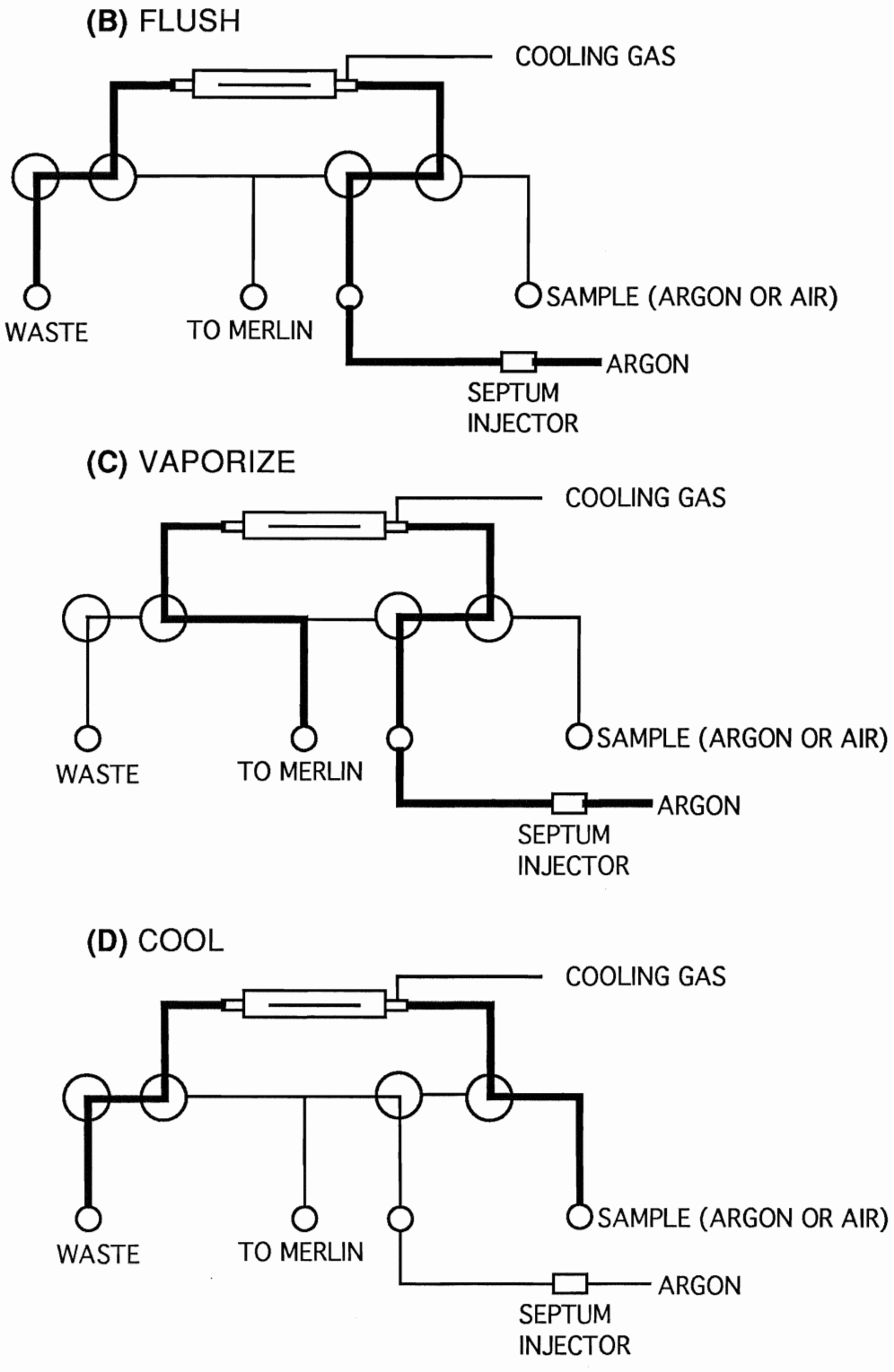

Figure 15 : Diagram illustrating the peristaltic pump sample delivery system and gas/liquid separator addition to the Galahad/Merlin system.

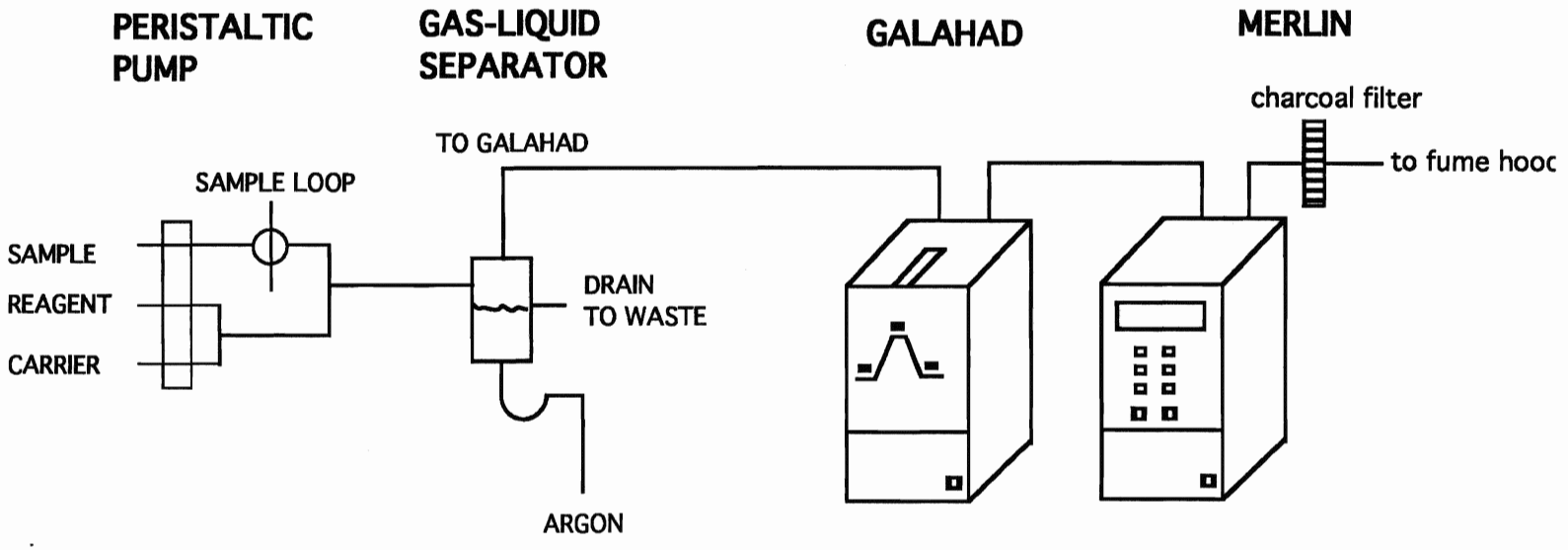

Figure 15 illustrates the peristaltic pump and gas/liquid separator addition.

An Alitea variable-speed two-piston sinusoidal flow pump (Alitea USA, P.O. Box 26, Medina, WA 98039) equipped with disposable syringes and rigid syringe plungers, and a Valco electronically actuated 8-position selection valve (figure 16) were employed in the sequential injection studies. A computer program was developed for integrated control of the pump, valve, Galahad, Merlin and recorder system.

Figure 16 : Diagram illustrating sequential injection and multi-position valve sample delivery system addition to the PSA Galahad/Merlin Mercury in water determination system.

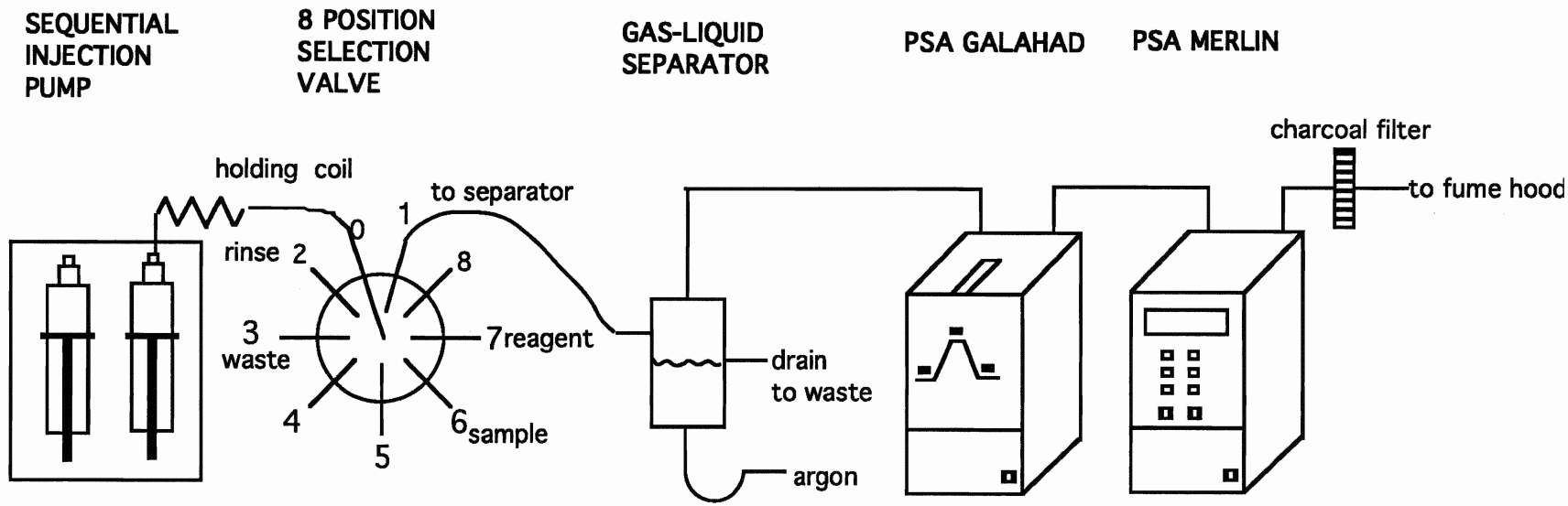

PROCEDURES

(A) CHLORIDE DETERMINATION

For all UV studies, Cl^-, $Hg(SCN)_2$, Fe^{3+} and KSCN solutions were pipetted from stock solutions into test tubes to produce desired concentrations for analysis. A continuous variation series of $Hg(SCN)_2$ and NaCl solutions were prepared, each containing a total sum molarity of NaCl + $Hg(SCN)_2$ of 2.2 $x10^{-3}$ M.

Flow injection studies on the Perkin Elmer flow system were performed by injecting various concentrations of chloride into a continuously flowing 0.012% m/v mercury thiocyanate carrier stream. The flow rate was maintained at 1.0 ml min^{-1} by the HPLC pump. Detector response at 254 nm was continuously recorded by a chart recorder from which peak heights, related to %transmission were obtained. Data were analyzed via Microsoft Excel and Cricket-Graph software.

Determinations on the in-house FIA system were performed by injecting chloride samples, via a manual switching valve, into the continuously flowing $Hg(SCN)_2$ carrier stream (0.023% or 0.035% m/v), propelled by a peristaltic pump. The sample plug moved to the detector through a knitted reactor (80 cm of 0.5 mm internal diameter tygon tubing) whereby mixing and interpenetration of the sample and carrier solution occurred. The flow rate was maintained at 1.2 ml min^{-1} by a peristaltic pump. Flow work was performed with both 1.0 mm i.d. Teflon tubing and 0.5 mm i.d. tygon tubing and the dispersion of each system was

determined by the injection of a sample loop volume of $Hg(SCN)_2$ into a water carrier stream and comparing the peak obtained, which has an absorbance at 254 nm, to the shift in absorbance when the flow cell was filled completely with the $Hg(SCN)_2$.

(B) MERCURY DETERMINATION

For mercury in air determinations on the original system, injections of mercury saturated air were performed via syringe to test reproducibility, response and peak quality. Mercury in water determinations were performed by delivering sample $HgCl_2$ and reagent $SnCl_2$ solutions to the gas/liquid separator, followed by aeration to deliver the Hg^0 plug to the Galahad. Preliminary work on mercury in air and water samples led to a series of primary changes to the system as obtained by PSA. These changes are listed as follows:

1. Decrease the diameter of the quartz tube surrounding the gold trap in the Galahad system.

2. Incorporation of leakproof teflon connectors from the quartz tube surrounding the gold mesh to the internal tubing of the Galahad.

3. Decrease the diameter of the tubing in the Galahad and the Merlin and change from tygon to teflon.

4. The gold mesh supplied as the gold trap was decreased to 1/4 its original size

5. A connection was made from the line of the sample inlet of the Galahad (from the gas/liquid separator) to a waste line.

After preliminary investigations involving both mercury injections in air and solution reactions, modifications of the valving system and flow paths of the Galahad were instituted. An experiment with this version of the system was performed to determine the concentration of Hg in laboratory air via standard addition. The peristaltic pump was set up to transport air at a rate of 50 ml min^{-1} directly to the Galahad. Air was sampled for a period of 2 min in the Amalgamation stage of the cycle, followed by manual activation of the series of Flush, Vaporize and Cool stages, and immediate syringe injection of a specified volume of Hg saturated air. Multiple injections of 0 (air alone), 5, 10, 15 and 20 µl of Hg saturated air samples were performed, and peak heights obtained were employed for regression calculations to determine the concentration of Hg in laboratory air.

Changes to the solution delivery system to the gas/liquid separator were made and involved:.

(1) Replacement of the peristaltic pump/manual switching valve system with a sequential injection pump/ electronically actuated selection valve for sample, reagent and wash solution delivery to the gas/liquid separator.

(2) A computer program was created[67] to control and integrate the solution delivery, Hg Amalgamation and Hg Determination cycles. The main features of the program include control of:

-cam driven sinusoidal flow pump
-sequential injector/selection valve and associated controls for reagent delivery to separator
-amalgamation and detection

-data acquisition and analysis, calibration curve
-parameter optimization
-intensive rinse cycle
-Galahad on flush cycle during inactive period

CHAPTER 3: RESULTS AND DISCUSSION

RESULTS AND DISCUSSION: CHLORIDE DETERMINATION

(A) EXAMINATION OF UTSUMI SYSTEM

Utsumi's method for chloride determination is based on the reaction of Cl^- with mercury thiocyanate to release thiocyanate ion which reacts with iron(III) to produce red $Fe(SCN)^{2+}$ that is detected at 450 nm. Examination of the dissociation constants of $Hg(SCN)_2$, $HgCl_2$, and $Fe(SCN)^{2+}$ raise an interesting question with respect to Utsumi's method. Based on these dissociation constants, it appears that the dissociation of $Hg(SCN)_2$ into Hg^{2+} and free SCN^- on page 21 should not proceed to the extent that it does. Preliminary experiments were performed using the visible/UV spectrometer in an attempt to examine the sequence of reactions of this method.

(1) A spectral (200-600 nm) scan of a series of solutions containing increasing concentrations of KSCN versus Fe^{3+} produced a series of peaks confirming that the species absorbing at 450 nm is indeed a complex involving Fe^{3+} and SCN^-. The addition of Cl^- to this series produced no effect on the spectra, eliminating the possibility that Cl^- is also involved in the absorbing complex.

(2) An experiment was performed where a series of spectral scans were obtained versus different reference solutions of a solution consisting of 0.01 M Fe^{3+}, 5.0×10^{-5} M $Hg(SCN)_2$, and 1.0×10^{-4} M Cl^-. This was done in an attempt to identify the wavelengths at which absorbance of intermediate complexes

may be occurring, such that these wavelengths may be examined at low concentrations to follow their increase. The reference solutions employed were (A) 0.01 M Fe^{3+}, (B) 0.01 M Fe^{3+}, 5.0 x 10^{-5} M $Hg(SCN)_2$, and (C) 5.0 x 10^{-5} M $Hg(SCN)_2$. Figure 17 illustrates the spectra obtained. Unfortunately, Fe^{3+} has a large absorbance in the 400-200 nm region, and because of this, it was virtually impossible to obtain any information with respect to the interactions occurring in solution in that spectral region. Examination of the scan reveals that when Fe^{3+} is included in the reference solution, a large negative peak appears in the region of ≈ 400-360 nm that appears to affect the absorbance observed at 450 nm. The occurrence of the negative peak is simply due to the fact that the concentration of free Fe^{3+} in the sample solution is less than in the reference solution, due to its reaction with liberated SCN^-. However, because this negative peak affects the peak observed at 450 nm, significant error due to variation in peak height may be introduced into the determination of Cl^- via this method, when Fe^{3+} is included in the reference solution.

(3) Other experiments performed to examine the interactions between $Fe^{3+}/Hg(SCN)_2/Cl^-$ included the determination of a calibration curve at 450 nm of Fe^{3+} (0.01 M - 0.1 M) versus constant concentration of $Hg(SCN)_2$. This experiment was undertaken because it was noticed in the previous series of experiments that when Fe^{3+} and $Hg(SCN)_2$ are combined in the absence of chloride ion, Fe^{3+} turns from yellow to slightly

Figure 17 : Spectral (200-500 nm) scans of a solution containing 0.01 M Fe^{3+}, 5.0 x10^{-4} M $Hg(SCN)_2$, and 1.0x10^{-3} M NaCl versus the following blanks: A, 0.01 M Fe^{3+}; B, 0.01M Fe^{3+} and 5.0x10^{-4} M $Hg(SCN)^2$; and C, 5.0x10^{-4} M $Hg(SCN)_2$ alone.

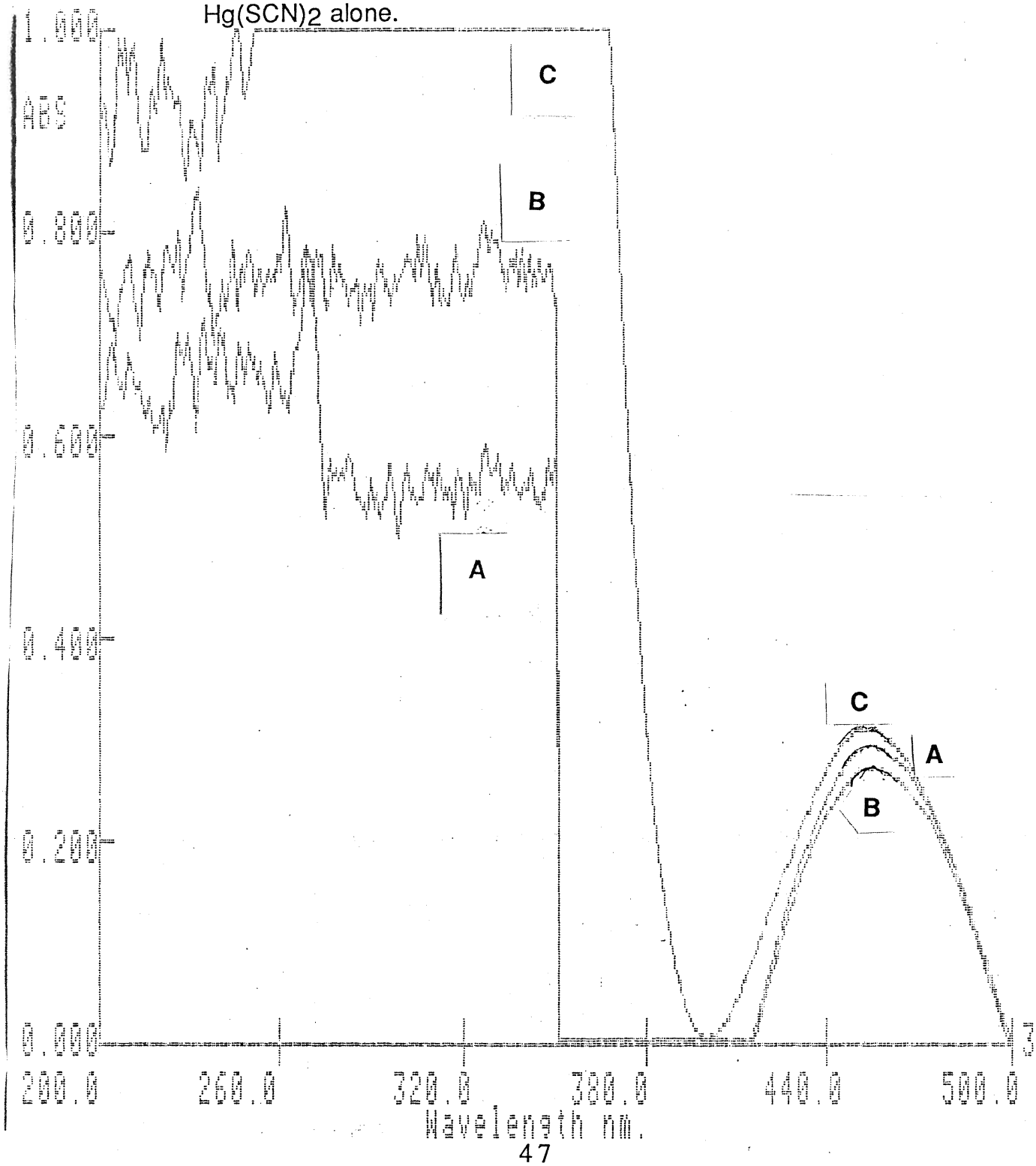

orange. Figure 18 shows that an increase in absorbance occurs with increasing Fe^{3+} concentration.

Figure 18: Plot of absorbance at 450 nm for increasing Fe^{3+} concentration versus constant 0.012% m/v Hg(SCN)2.

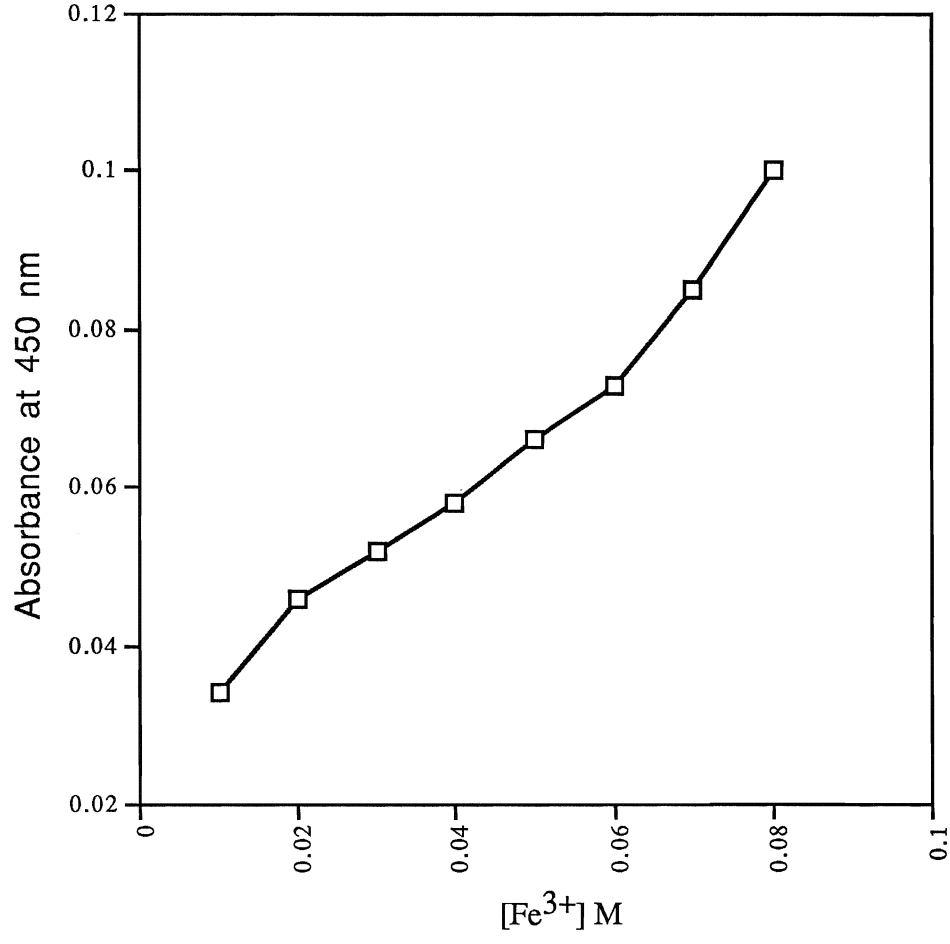

The results of this experiment are puzzling when the dissociation constant of $Hg(SCN)_2$ is considered. According to equation 7, there should be very little SCN^- in solution. The possibility the presence of free SCN^- as a result of the

manufacture of the $Hg(SCN)_2$ reagent, was considered and a saturated stock solution was prepared from leached $Hg(SCN)_2$. A comparison of the plots of $[Fe^{3+}]$ versus $[Hg(SCN)_2]$ employing both the treated and original $Hg(SCN)_2$ revealed no difference in response between the $Hg(SCN)_2$ solutions. These results eliminated the possibility of free SCN^- being present in solution due to manufacturing processes but did not explain the phenomenon. Thus the interaction is not due to excess SCN^-, but it does occur both in the absence of Cl^- and in the presence of Cl^- (to a greater extent in this case).

The occurrence of absorbance at 450 nm for the plot of $[Fe^{3+}]$ versus $[Hg(SCN)_2]$, led to the question of whether absorbance would be observed at 450 nm when Fe^{3+} concentration is maintained constant while $Hg(SCN)_2$ is varied. **(4)** A plot of $[Hg(SCN)_2]$ versus $[Fe^{3+}]$ was obtained and compared to one produced in the presence of chloride. Figure 19 reveals that a constant low absorbance is observed at 450 nm in the absence of chloride ion, whereas a positive slope is observed in the presence of chloride ion. This slope does appear to level off as concentrations approach the 100 $\mu g\ ml^{-1}$ Cl^- level, consistent with the limitation of low linear range, previously described for Utsumi's method.

The behaviour experienced at 450 nm with increasing $[Fe^{3+}]$ versus constant $[Hg(SCN)_2]$ (figure 18) is similar to what occurred in the presence of increasing chloride concentration versus constant $[Fe^{3+}]$ (figure 19). Comparison of these results has led to the conclusion that the

$Fe(NO_3)_3 \cdot 9H_20$ reagent obtained from BDH contained Cl^-. This may explain why there was an increase in absorbance at 450 nm when Fe^{3+} was varied versus $Hg(SCN)_2$ but no increase when $Hg(SCN)_2$ was varied versus Fe^{3+}.

Figure 19 : Comparison of absorbance curves of constant 0.01 M Fe^{3+} and varying SCN^- (from $(HgSCN)_2$) to 0.01 M Fe^{3+} and varying SCN^- and Cl^- (from $Hg(SCN)_2$/NaCl solutions).

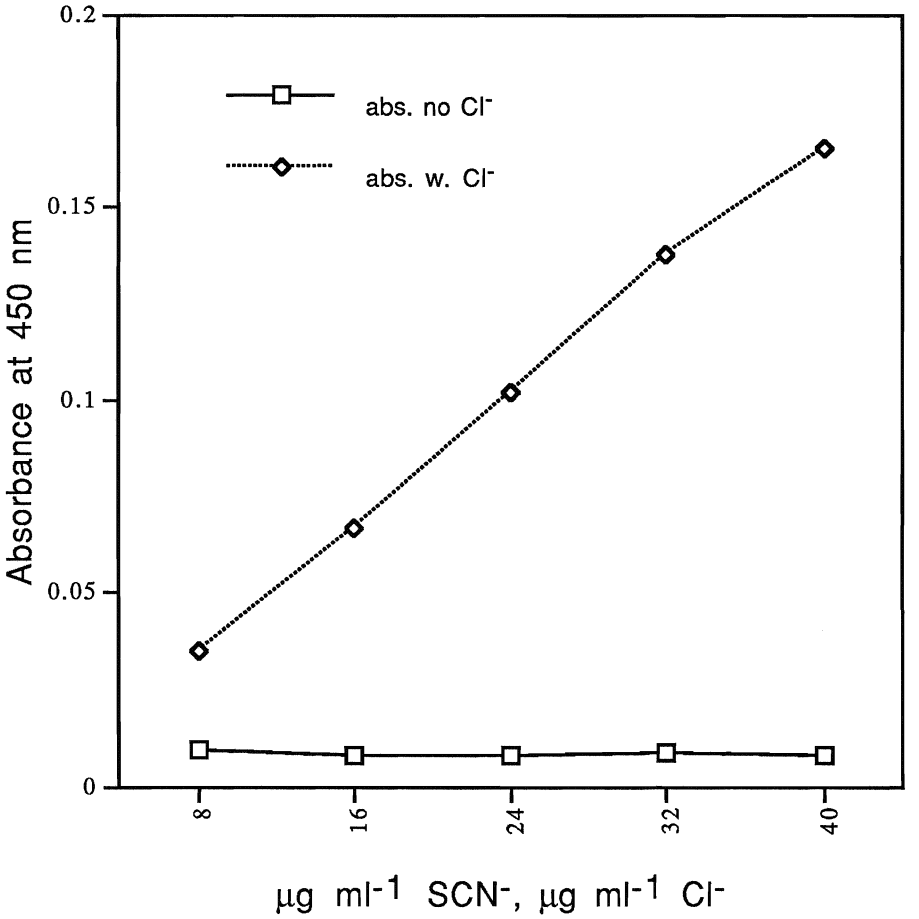

* µg ml^{-1} SCN^- in solution if $Hg(SCN)_2$ were to completely dissociate.

(B) DISCOVERY OF 250 nm PEAK

Continuing the search for information of the interactions between the analytes involved in Utsumi's method, an investigation into the interaction between Cl^- and $Hg(SCN)_2$ in solution was performed. A calibration experiment of Cl^- versus $Hg(SCN)_2$, in the absence of iron(III) revealed a relatively intense peak in the 250-260 nm region that increases with added chloride (figure 20). The appearance of this peak at 250 nm suggests that an interaction occurs between chloride ion and mercury thiocyanate in solution. A continuous variation experiment was performed to examine the stoichiometric association between Cl^- and $Hg(SCN)_2$ in solution and figure 21 shows that the maximum absorption occurs at a stoichiometric ratio of approximately $2Hg(SCN)_2$:1NaCl in solution. This suggests that the association may involve a chloride ion bridging two $Hg(SCN)_2$ molecules in solution. It is not clear whether this peak occurs when iron(III) is present due to the large absorbance by Fe^{3+} in the 250 nm region, and thus it cannot be confidently stated whether a similar reaction occurs in Utsumi's $Fe^{3+}/Hg(SCN)_2/Cl^-$ system.

The discovery of the intense peak at 250 nm suggested that it might be used as an alternate means for chloride determination. Responses at 250 nm and at 450 nm were investigated and compared. Calibration experiments for chloride ion detection at 450 nm with $Hg(SCN)_2$ /iron(III) and

at 250 nm with $Hg(SCN)_2$ were performed. Figure 22 illustrates the response curves obtained. The response curve for 250 nm clearly exhibits greater sensitivity than that produced at 450 nm. The results of this experiment justified further study of this response as a possible alternate method for chloride analysis in water.

Figure 20 : Rise in absorbance in 250 nm region with increase in Cl^- concentration for solutions containing 0.012% $Hg(SCN)_2$.

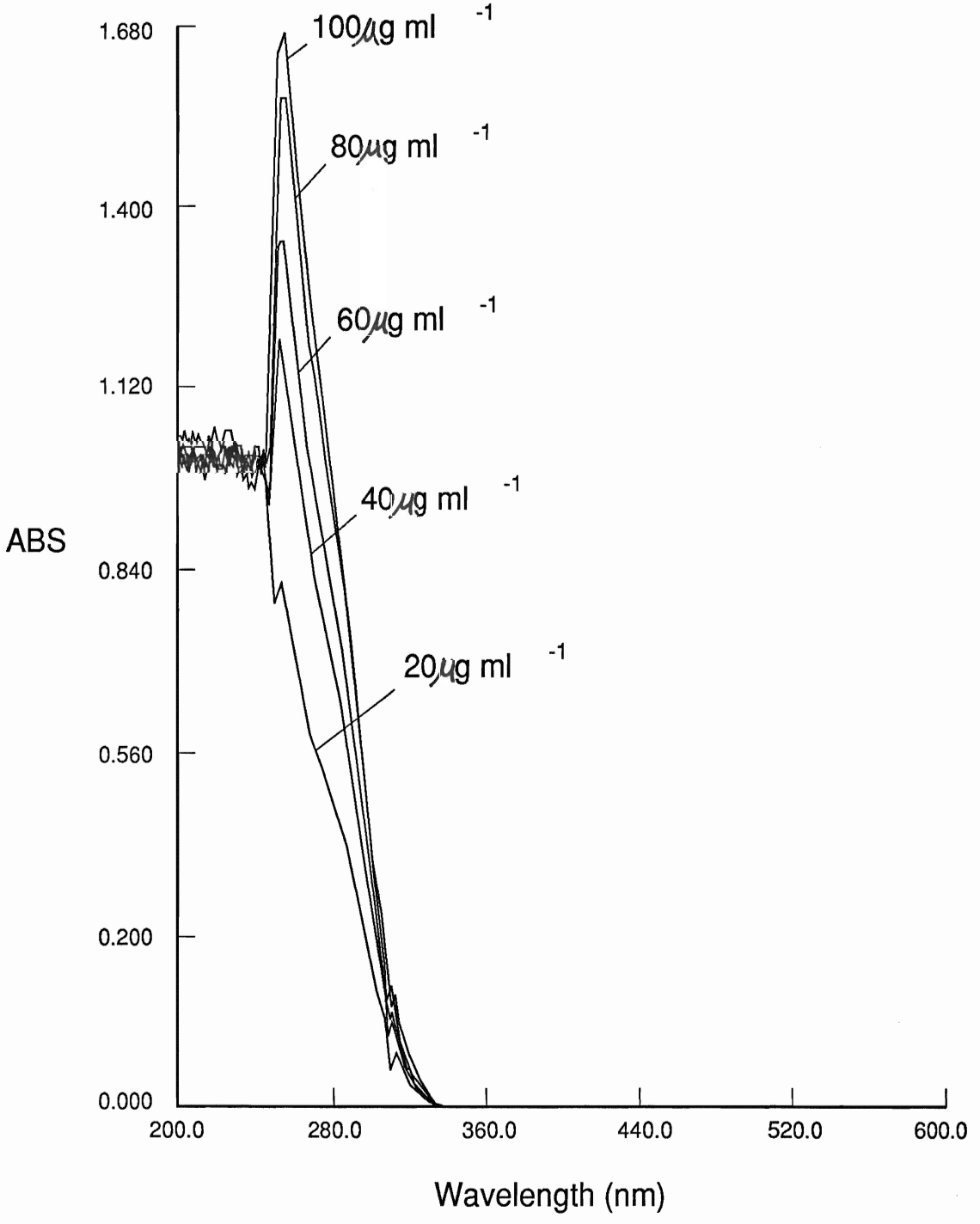

Figure 21: Molarity concentration comparison between $Hg(SCN)_2$ and Cl^-. Increments of 2.2 $x10^{-4}$ M with total molarity contributions from $Hg(SCN)_2$ + Cl^- equaling 2.2 $x10^{-3}$ M.

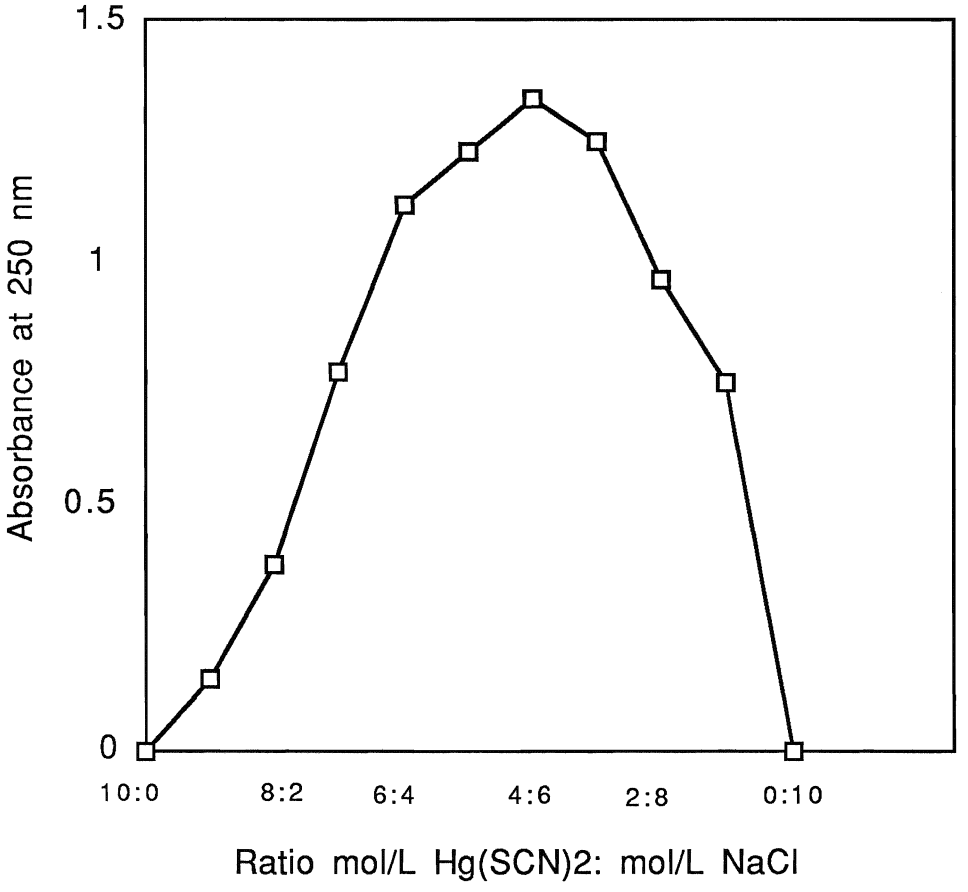

Figure 22: Comparison of absorbance at 250 nm for $Hg(SCN)_2$ reagent and at 450 nm for $Fe^{3+}/Hg(SCN)_2$ solutions with increasing chloride concentration.
—□— : absorbance at 250 nm;
—◊— : absorbance at 450 nm.

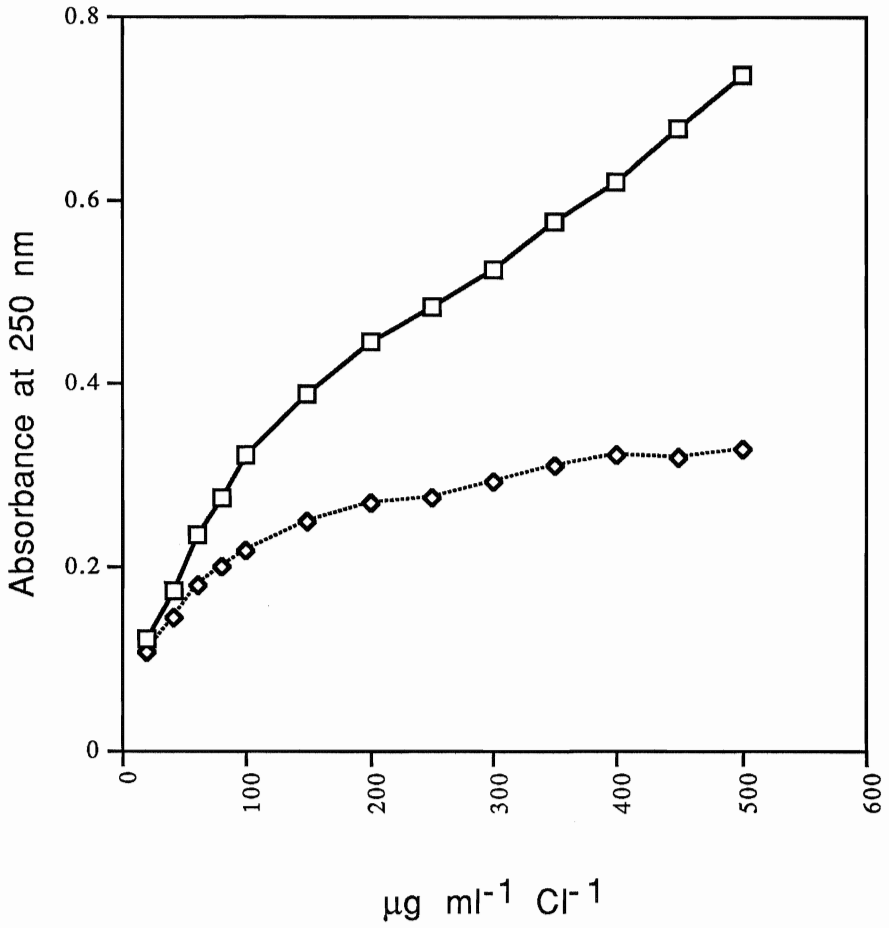

(C) CONTINUOUS FLOW WORK ON PERKIN ELMER SYSTEM

Studies with the $Hg(SCN)_2/Cl^-$ system were continued with a continuous flow FIA setup on the Perkin Elmer HPLC instrument. The study of the 250 nm response was easily adapted to continuous flow methods and the use of FIA demonstrated several advantages over the manual batch methods employed for the UV-vis spectrophotometric studies. These included much improved time efficiency of analyses. For example, a calibration on the spectrophotometer required the preparation of many solutions containing varying aliquots of manually pipetted solutions. Opportunities for error abound here (ie. pipet handling, transfer to test tube, switching of test tubes etc.). These sources of error are all but eliminated if FIA is employed. Stock solutions or their appropriate dilutions are transported through the system to the detector without human intervention other than the manual switching of the valve diverting the sample loop into the carrier stream. As mentioned in the introduction, each sample is processed in exactly the same way during its transport to the detector, resulting in excellent reproducibility of detector response.

(A) The first experiment on the Perkin Elmer system involved the injection of chloride into a $Hg(SCN)_2$ carrier stream. Figure 23 illustrates the response at 254 nm obtained. For concentrations of injected chloride below 200 $\mu g\ ml^{-1}$ negative peaks were observed; double peaks were observed at high concentrations (figure 24). As $Hg(SCN)_2$

absorbs at 254 nm, the occurrence of negative peaks is due to dilution of the carrier stream with the sample plug. Double

Figure 23: Plot of response at 254 nm for chloride injected into 0.012% m/v $Hg(SCN)_2$ carrier stream on Perkin Elmer HPLC instrument.

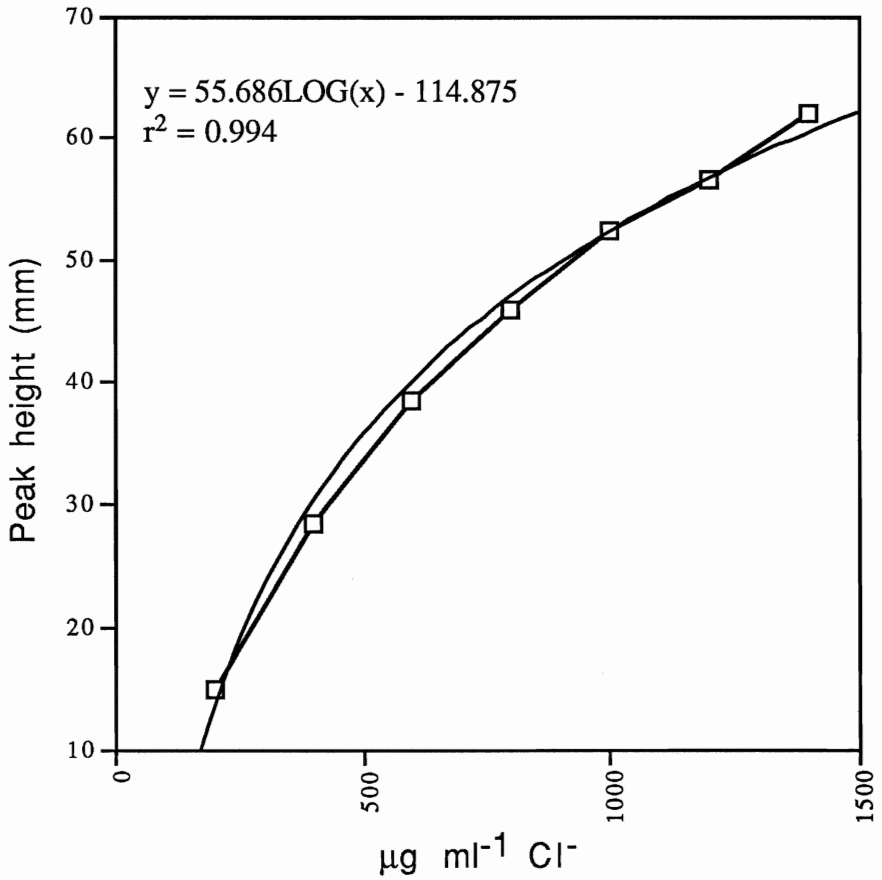

peaks were believed to be due to the very small internal diameter of the stainless steel tubing of the HPLC which limited mixing between the analyte and the reagent. The

system as employed was not homogeneous in the diameter of tubing connecting the HPLC pump to the sample loop to the detector. The diameter of the microreactor region (i.e. the region between the sample injection port and the detector) was less than 0.25 mm, smaller than the diameter of tubing typically employed for limited dispersion experiments. Thus this system was causing the sample plug to occupy a long length of tubing while restricting the contact between the carrier reagent and sample zones. It was for this reason that the setup of an in-house FIA system became necessary to facilitate the manipulation of tubing connections between the sample injection port and the detector, to control the dispersion of the system, and to place a knitted reactor into the line.

Figure 24 : Chart recorder printouts of chloride injections (10 µL) into 0.012% m/v Hg(SCN)2 carrier stream. Detection at 254 nm.

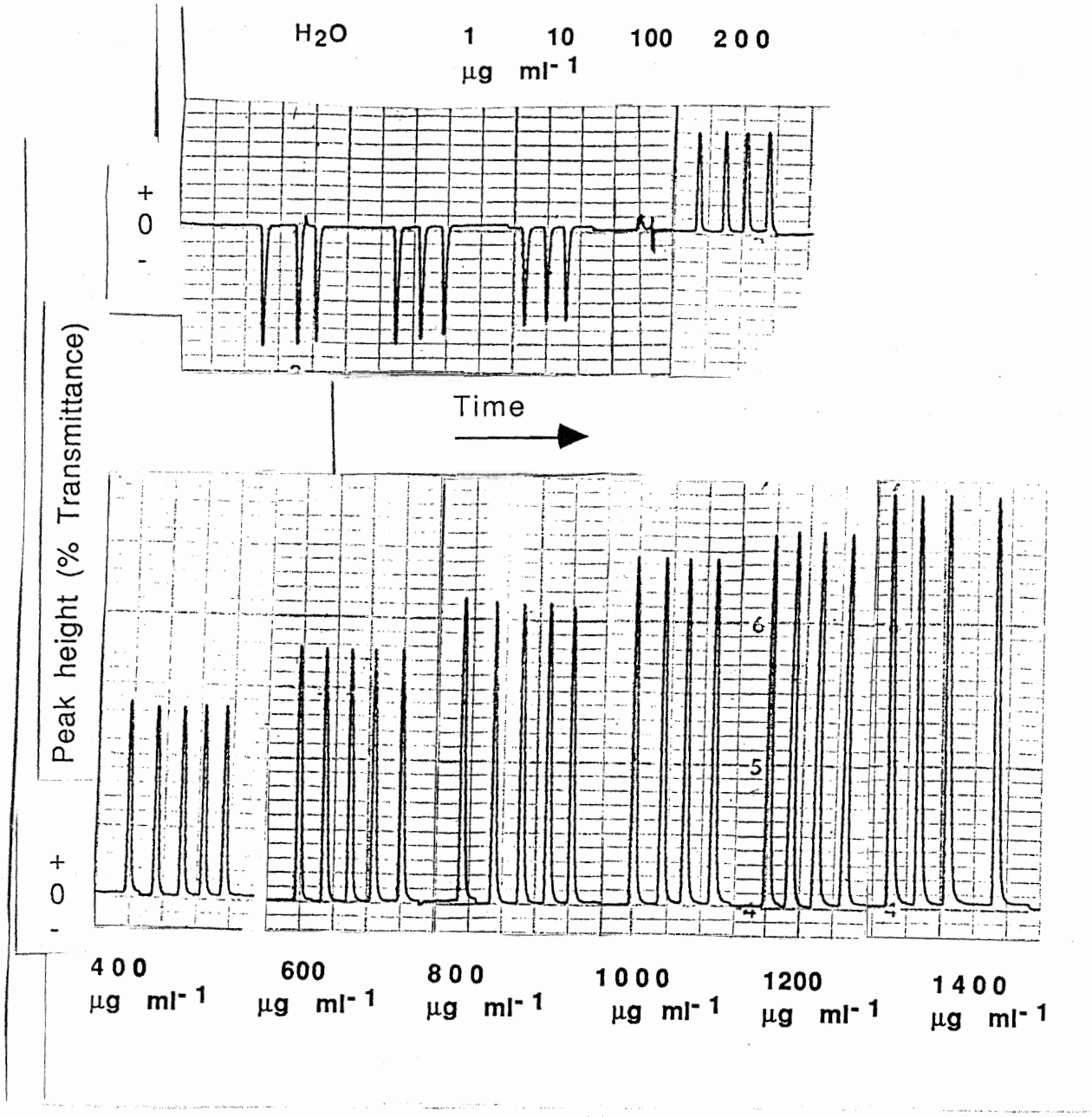

(D) FLOW INJECTION ANALYSIS ON IN-HOUSE SYSTEM

The in-house FIA system consisted of a peristaltic pump, a switching valve, and a flow-through cell placed in the optical path of an FAAS system. The construction of this system is a wonderful example of how simple and economical it is to automate a method employing FIA.

(1) A calibration curve (fig. 25) of chloride injected into the $Hg(SCN)_2$ carrier stream revealed that absorbance at 254 nm increases with increasing Cl^- concentrations up to 3000 $\mu g\ ml^{-1}$. Curve-fitting revealed that a logarithmic relation exists between the chloride concentration injected and peak height obtained. A plot of log[Cl^-] versus peak height produced a straight line which is illustrated in figure 26. Negative peaks were obtained for concentrations below 20 $\mu g\ ml^{-1}$ but if the negative peak value for H_20 is assigned a value of zero, a linear calibration curve is obtained of chloride concentration versus peak height for values of 0-40 $\mu g\ ml^{-1}$ Cl^- (figure 27). Figure 28 illustrates the excellent peak quality and reproducibility obtained by this system.

The linear relationship between log concentration and recorder output demonstrates a deviation from Beer's law of $Abs = \varepsilon bc = -\log I/I^o = \log 1/T$, where I/I^o represents transmission. The detector of the optical system employed in the in-house FIA system generated signals from percent transmission from the flow-through cell. If the system obeyed Beer's Law, a linear relationship between log[peak height] and

concentration would have been observed, but because this was not observed, it can be concluded that the absorbing system of $Hg(SCN)_2$ and Cl^- at 254 nm does not obey Beer's Law. A cause for this may be that reagent $Hg(SCN)_2$ is completely consumed as high levels of chloride are introduced into the system.

Figure 25: Plot of peak height obtained at 254 nm for chloride injected into 0.024% m/v $Hg(SCN)_2$ carrier stream on in-house FIA system.

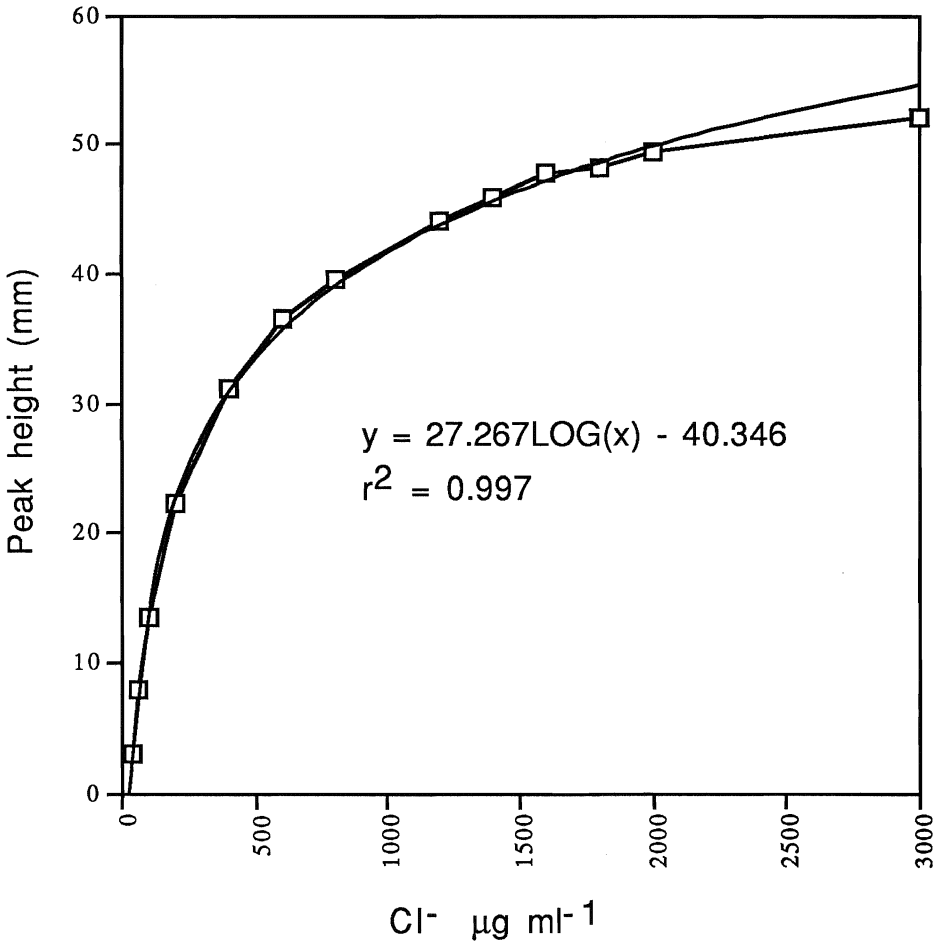

Figure 26: Plot of peak height versus log[µg ml^{-1} Cl^-] for chloride injected into 0.024% m/v $Hg(SCN)_2$ carrier stream on in-house FIA system.

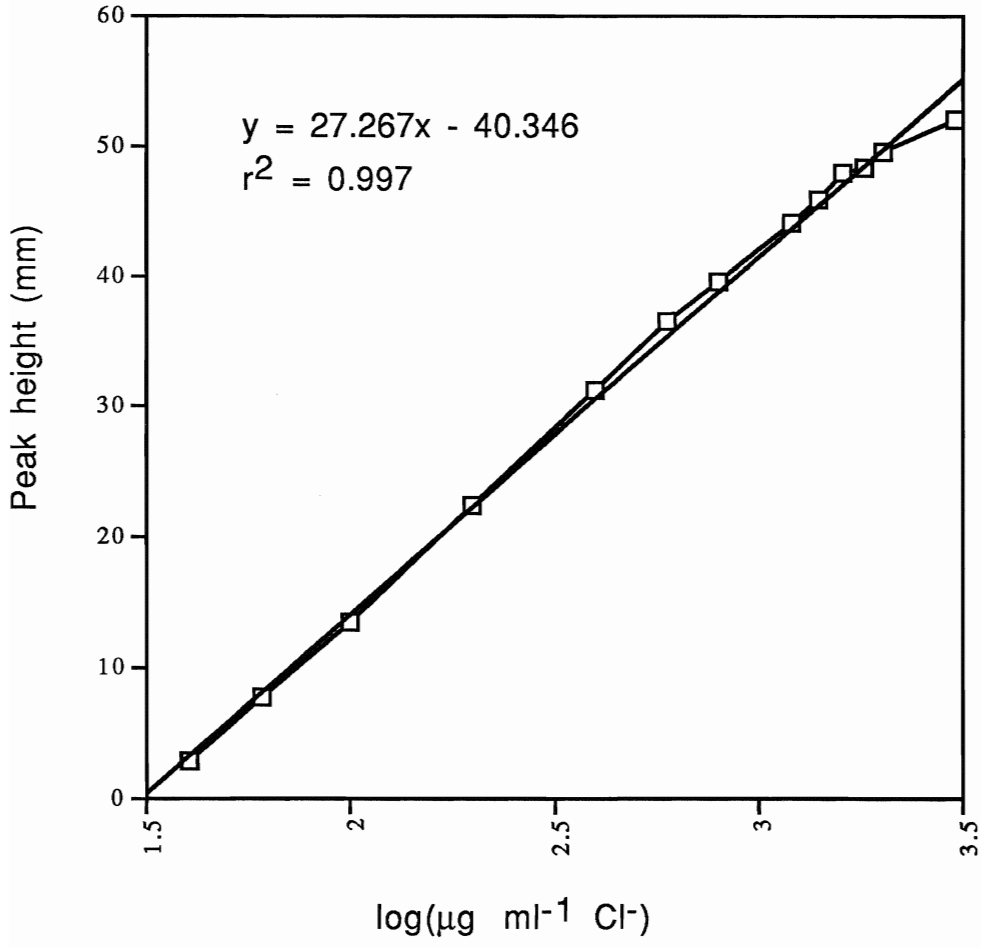

Figure 27: Plot of peak height (relative to blank H_2O peak height) versus µg ml^{-1} Cl^- injected into 0.024% m/v $Hg(SCN)_2$ carrier solution.

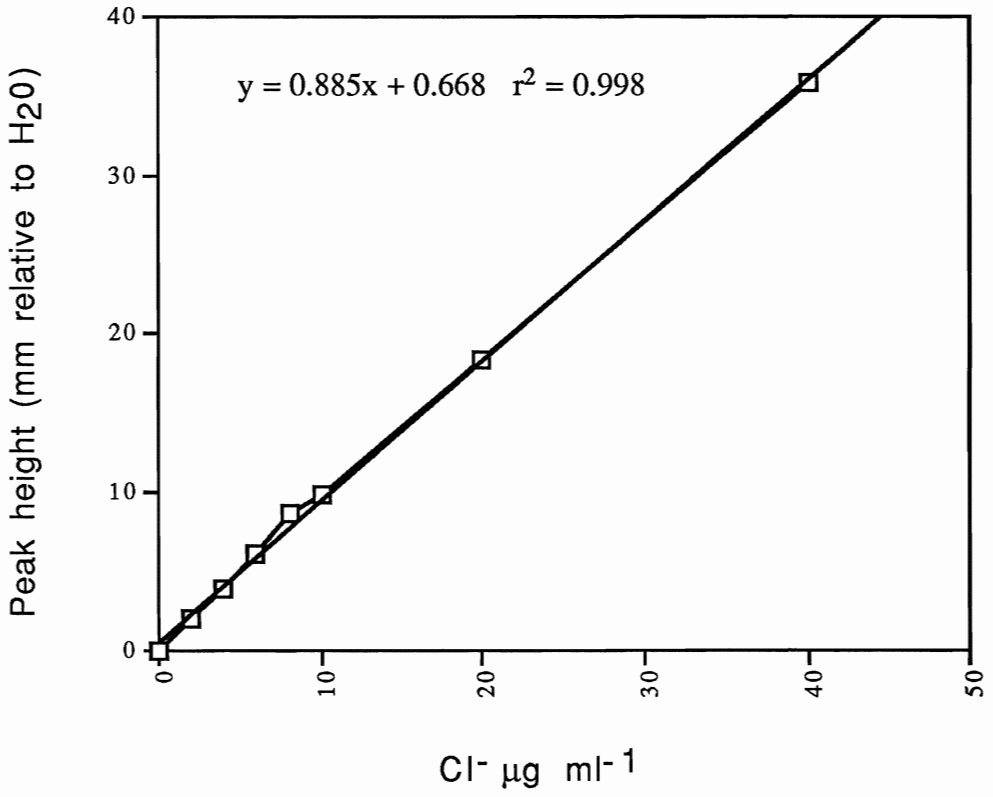

Figure 28 : Recorder plots of peaks obtained with chloride sample injections into the in-house FIA system (0.024% m/v $Hg(SCN)_2$ carrier stream, 10 µl sample loop).

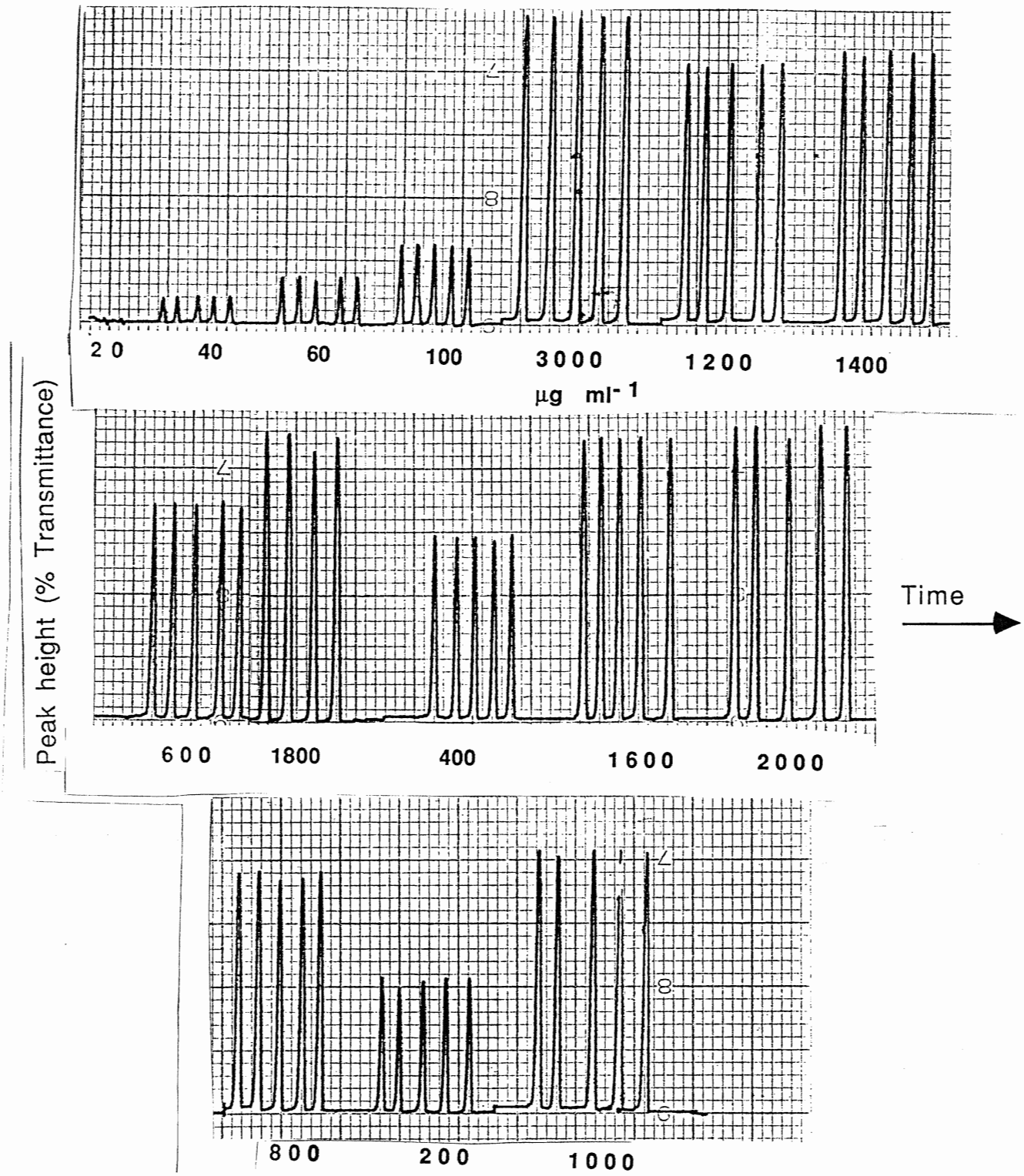

(2) The dispersion of the system setup employed for the previously mentioned data was determined. Figure 29 illustrates the peak heights obtained from the injection of 10 µl of $Hg(SCN)_2$ and the height produced when the flow cell is completely filled with the same solution. Substitution of the peak height values into equation 1 produced a D value of 11, corresponding to high dispersion. This D value indicates that the sample plug is diluted 11 times by the carrier solution, indicating that it is spread out over a significant distance within the tubing of the system. Examination of the system revealed that there were areas that could be modified to decrease the dispersion of the sample plug and thus decrease the peak width and increase the peak height. The most important area of modification was the line connecting the switching valve to the knitted reactor to the flow-through cell, as this is where the absorbing species is produced and transported to the detector. Originally, this line consisted of a short length of Teflon 0.5 mm i.d. tubing connected to the knitted reactor (1.0 m x 1.0 mm i.d.) which was fitted over the inlet of the flow-through cell. Connections can produce local areas of turbulence, resulting in spreading of the sample plug. This line was replaced by one continuous length of 0.5 mm i.d. tygon tubing from the switching valve to the flow-through cell. The internal diameter of the tubing was decreased from 1.0 mm, as commonly employed for large dispersion to 0.5 mm to create a medium dispersion system and also to improve the reagent economy of the system.

Figure 29(B) illustrates the injections performed to measure the dispersion of the modified system, determined via equation 1 to be D=3 (medium dispersion). Improvements noticed with the modified system included an increased sharpness of peaks and a decreased sampling time. A comparison of the peaks obtained with the D=11 system (fig 28) to those obtained with the D=3 system (fig 30) clearly reveals the improvement. The sampling time of the large dispersion system was on the order of 60 s whereas a cycle with the medium dispersion system is complete within 30 s, indicating a sampling frequency of 120 samples/hour. This medium dispersion system was employed in the remainder of experiments.

Figure 29 : Plots of dispersion determinations performed for the in-house FIA system. A reveals high dispersion, D=11 and B demonstrates medium dispersion, D = 3.

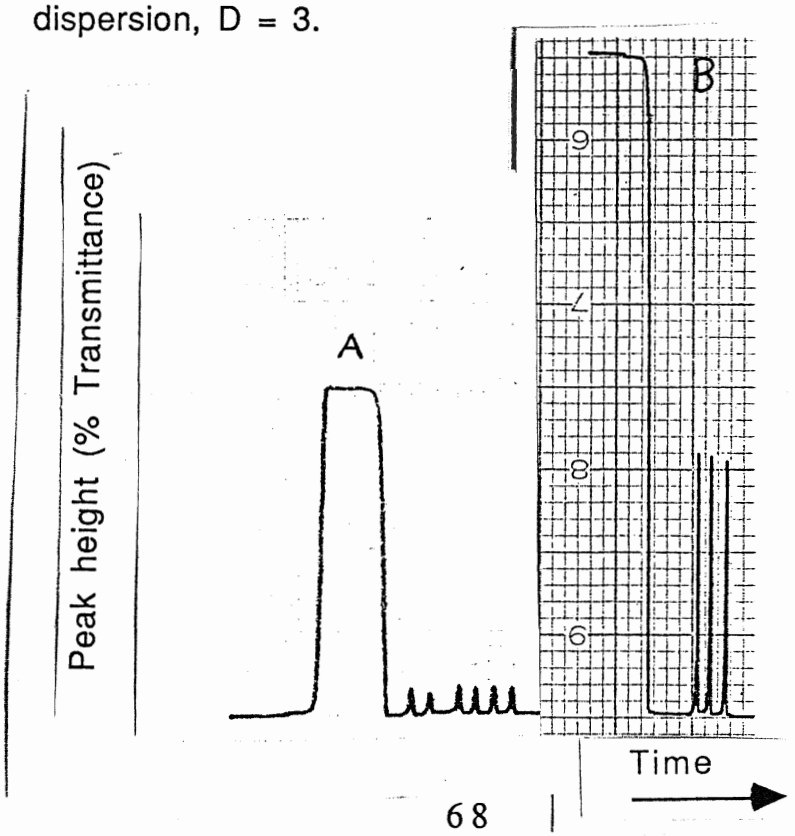

Figure 30: Plots of detector response for chloride injections into D=3 medium dispersion system (0.036% m/v $Hg(SCN)_2$ carrier stream, 10 µl sample loop).

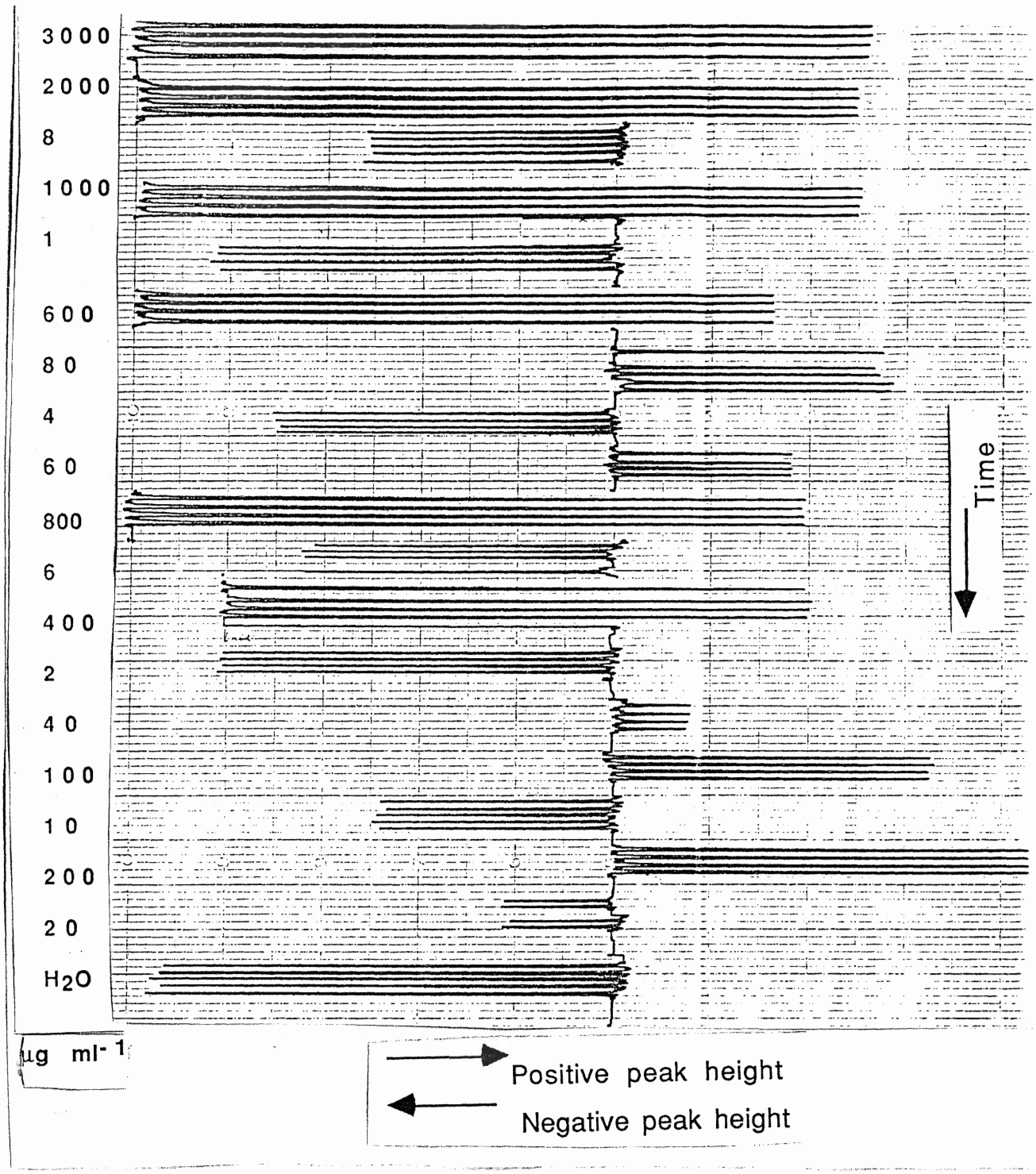

DETECTION LIMIT

The detection limit of this system was determined according to the IUPAC method (three times the standard deviation of a series of 23 blank injections) and was found to be 0.16 μg ml^{-1} Cl^-. Where the injected chloride concentration gave a response close to the transition from negative to positive peaks, a small double peak was often observed (figs. 24,28 and 30). It is believed these perturbations may be due to the difference in refractive index between the sample and carrier solution zones that result in the distortion of the light beam as it passes through the photometric cell.[70]

APPLICATION: DETERMINATION OF CHLORIDE CONCENTRATION IN LABORATORY TAPWATER

A standard addition method was employed to determine the concentration of Cl^- in laboratory tap water. Employing concentrations of 50, 100, 150, and 200 μg ml^{-1} added chloride ion, the Cl^- ion concentration in tap water was determined to be 24.0 ± 0.6 μg ml^{-1}. An analogous batch experiment performed with the $Hg(SCN)_2/Cl^-/Fe^{3+}$ system at 450 nm on the UV visible spectrophotometer yielded 26 ± 1 μg ml^{-1} Cl^- in the same tapwater sample. An F-test and a t-test performed on the results of the two methods proved them to be indistinguishable at the 99% level of confidence. Figures 31 and 32 illustrate the linear log plots obtained for the standard addition analysis by the two methods and tables 1 and 2 list the statistical data.

Table 1 : F-TEST DATA EMPLOYED TO COMPARE PROPOSED FIA METHOD TO CLASSICAL UV-VIS BATCH METHOD (from reference 68).

Mean rsd for Fe^{3+}/ $Hg(SCN)_2/Cl^-$ system (on UV-vis)	0.039
Mean rsd for proposed FIA method	0.026
Critical F value* for 99% confidence level	3.52

*[based on 20(#samples)-5(#concentrations)= 15 deg freedom in both numerator and denominator]

$F_{exptl.}$ = larger variance/smaller variance

$= (0.039)^2/(0.026)^2$

$= 2.25$

Thus $F_{exptl.} < F_{crit.}$ indicating there is no difference between the two methods.

Table 2 : t-TEST DATA EMPLOYED TO COMPARE PROPOSED FIA METHOD TO CLASSICAL UV-VIS BATCH METHOD (from reference 69).

Mean rsd for Fe^{3+}/ $Hg(SCN)_2/Cl^-$ system (on UV-vis)	x_1= 0.039
Mean rsd for proposed FIA method	x_2= 0.026
pooled s value for both methods	s =0.0482
t value* for 99% confidence level	t = 3.36

$$x_1 - x_2 = 0.039 - 0.026 = 0.01314$$

$$\pm ts \sqrt{(N_1+N_2/N_1N_2)}$$

$$3.36(0.0482)\ [\sqrt{(5+5/5x5]}$$

$$\pm 0.1024$$

Thus, $x_1 - x_2 < \pm ts \sqrt{(N_1+N_2/N_1N_2)}$, supporting the null hypothesis that there is no difference between the two methods.[69]

Figure 31: Standard addition plot of peak height vs log[10+μg $ml^{-1}Cl^-$]* for Cl^- added to solutions containing laboratory tapwater. Chloride concentration in tapwater determined via proposed FIA method: $[Cl^-]$ = 24.0 ± 0.6 μg ml^{-1}.

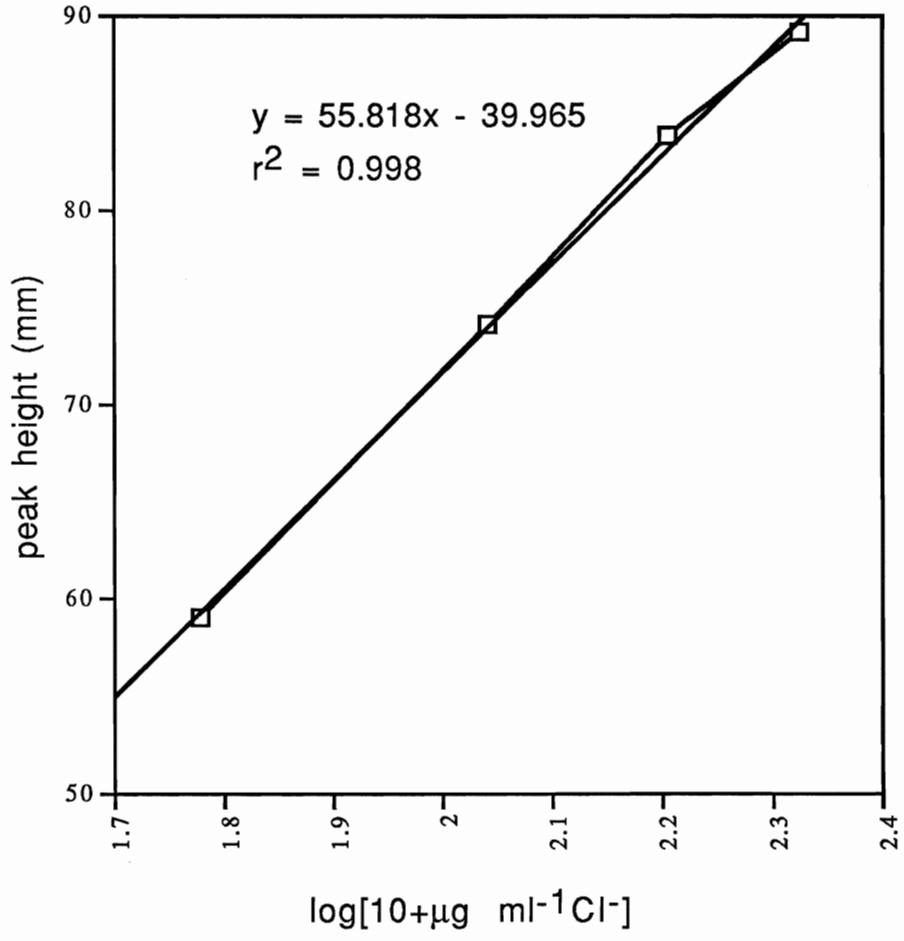

*note that the x axis is log[10+μg ml-1 Cl-], the arbitrary value of 10 was added to the concentrations of the standard addition to avoid a log[0] term for the 0 added Cl^- point.

Figure 32: Plot of absorbance at 450 nm versus log[10 + μg ml^{-1} Cl^-]* for Cl^- added to solutions containing Fe^{3+}, $Hg(SCN)_2$, and tapwater for standard addition. Chloride concentration in tapwater determined via conventional spectrophotometric method: $[Cl^-] = 26 \pm 1$ μg ml^{-1}.

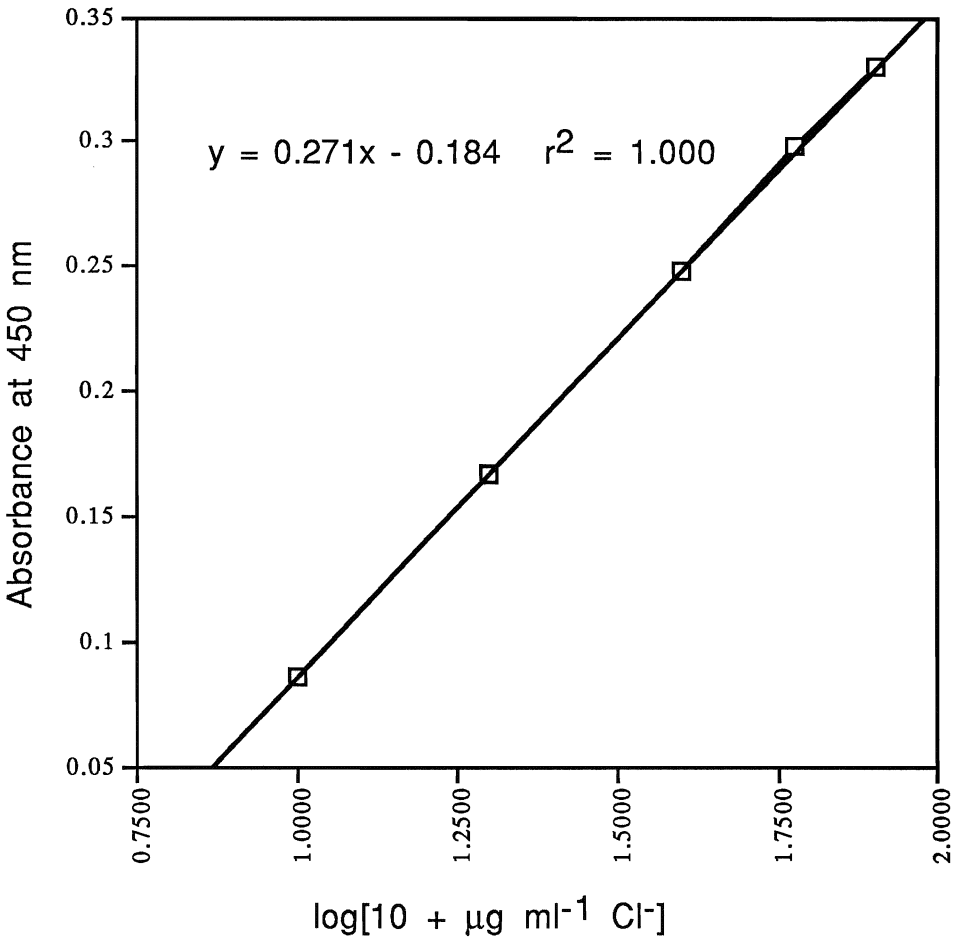

*note that the x axis is log[**10**+μg ml-1 Cl-], the arbitrary value of 10 was added to the concentrations of the standard addition to avoid a log[0] term for the 0 added Cl^- point.

INTERFERENCES

Interference studies were performed to examine which ions, commonly found in water, interfere with the determination of chloride. The presence of sulfide and carbonate ions in water was eliminated by the acidification of the solutions with HNO_3. The interference of sulphate ion, cations Mg^{2+} and Ca^{2+}, and anions Br^- and I^- on chloride determination were tested. Interfence of concentrations of 10, 20, 50, 70 and 100 $\mu g\ ml^{-1}$ of the various ions on signals from 100 $\mu g\ ml^{-1}$ chloride solution was investigated. It was found that SO_4^{2-}, Mg^{2+} and Ca^{2+} do not interfere with the signal from 100 $\mu g\ ml^{-1}$ chloride, over the concentration range of 0-100 $\mu g\ ml^{-1}$ interferent. However, bromide and iodide ion interfere with chloride determination at 254 nm. The presence of Br- from concentrations of 10 up to 100 $\mu g\ ml^{-1}$ resulted in proportionately enhanced peak heights for 100 $\mu g\ ml^{-1}$. Iodide interference occurs with an initial depression (10%) of the 100 $\mu g\ ml^{-1}$ signal for 10 $\mu g\ ml^{-1}$ added I^- and enhanced signals for 20 to 100 $\mu g\ ml^{-1}$ iodide interferent (figure 33). The interference of other halogen ions with the determination of chloride ion is not surprising as Br^- and I^- are known[17] to compete with Cl^- for $Hg(SCN)_2$.

Figure 33 : Plots illustrating effect of added Br^- and I^- interferents on peak height of 100 μg ml^{-1} Cl^- injected into 0.036% m/v $Hg(SCN)_2$ carrier stream.

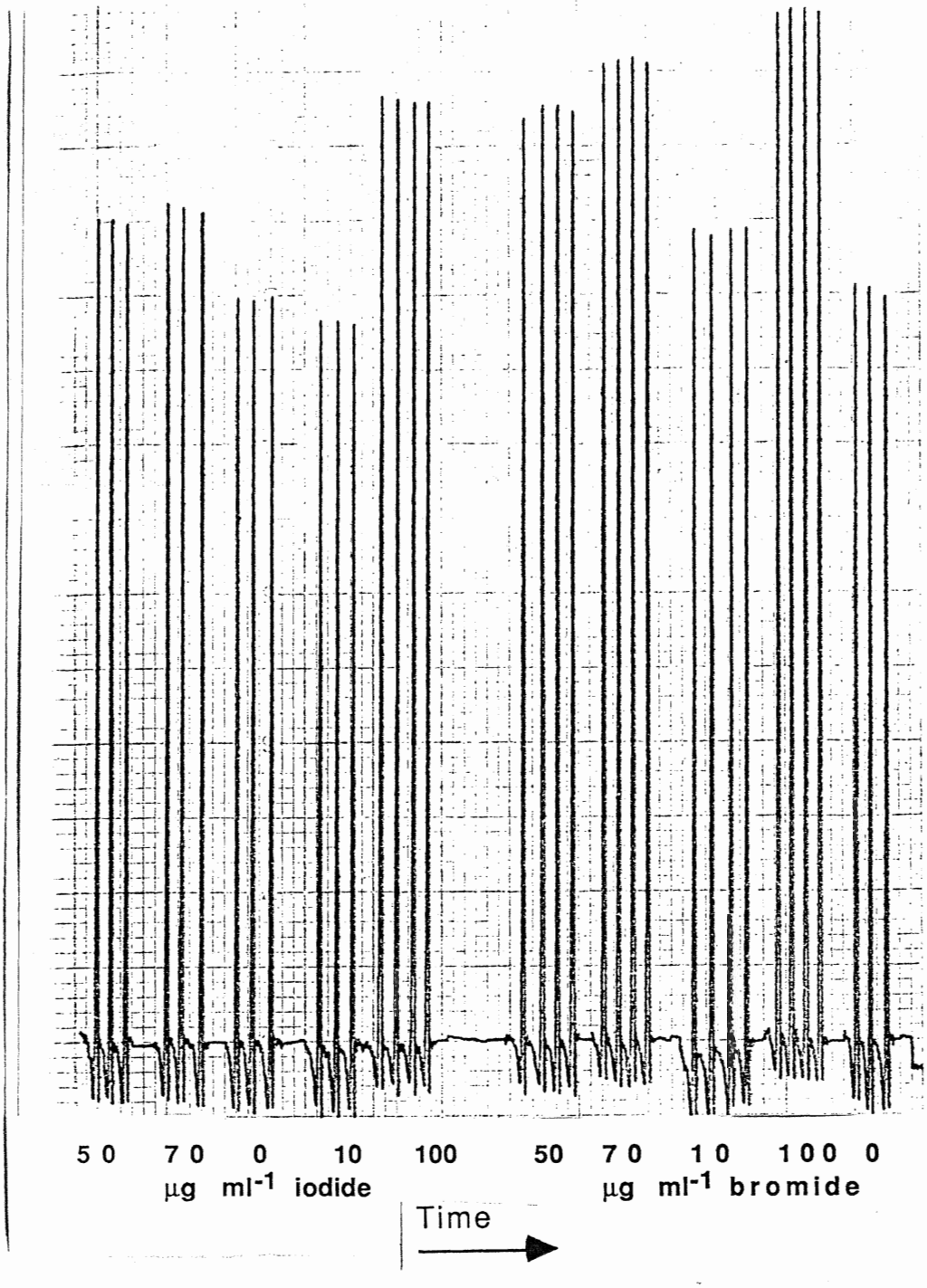

CONCLUSIONS: CHLORIDE DETERMINATION

Examination of Utsumi's chloride determination system at 450 nm involving $Fe^{3+}/Hg(SCN)_2/Cl^-$ has revealed that the absorbing complex at 450 nm is indeed $Fe(SCN)^{2+}$. The dissociation constants for $Hg(SCN)_2$ and $HgCl_2$ (equations 7 and 8) indicate that $Hg(SCN)_2$ should not dissociate in solution to provide a significant concentration of free SCN^- to react with iron(III). However, this reaction does occur in the presence of chloride ion and the reason for this occurrence is still unknown.

Absorbance was observed at 254 nm for the system involving Cl^- and $Hg(SCN)_2$, which exhibited a linear log relation from essentially 0 to 2000 μg ml^{-1} injected chloride. This linear range spanning three orders of magnitude is superior to the $Hg(SCN)_2/Cl^-/Fe^{3+}$ system, which exhibits much lower sensitivity and can only be confidently applied to determine chloride ion in the concentration range of 0.1-20 μg ml^{-1}.[10] Although the iron(III)/$Hg(SCN)_2/Cl^-$ system may adequately be employed for low chloride concentration determination, its application to determination of chloride concentrations above 100 μg ml^{-1}, where the slope of the calibration curve is very close to zero, requires dilution of the sample.[9-15] It is for this reason that the technique which employs 254 nm for the chloride/mercury thiocyanate complex appears to be superior. The system was successfully employed for the determination of chloride in laboratory tapwater in an

experiment which also demonstrated the practical advantages of automation over manual batch methods. Cations did not interfere with chloride determination in water whereas other halogen ions, I^-, Br^- did affect the determination of chloride.

Although the proposed method still employs toxic mercury thiocyanate, the use of FIA minimizes risks of exposure due to minimal opportunities for contact.

RESULTS AND DISCUSSION: MERCURY DETERMINATION

The main focus of the research employed with the PSA Galahad/Merlin system has involved the optimization and adaptation of the sytem to determinations of mercury in solution. Many modifications have been made to the original system obtained from PSA Analytical and they can be categorized into three subgroups. The first series of modifications involved changes to the internal hardware of the Galahad and Merlin systems, the second group included modifications to the internal valving system of the Galahad and, the third series of modifications involved the implementation of computer control and changes to the reagent delivery system.

Initial work with the PSA Galahad/Merlin system as obtained from PSA Analytical involved injections of mercury saturated air into the Galahad or mercury solutions to the separator, followed by manual activation of the Flush, Vaporize and Cool cycles during which time detector response was recorded on a chart recorder as peak heights. Poor reproducibility of the system and significant blank peaks were observed, making it quite difficult to obtain satisfactory data for analysis. Difficulty in stabilizing the system was also experienced and an investigation into the causes of this instability was undertaken. It was believed that poor reproducibility was due to: (1) insufficient cooling of the gold trap before initiation of the next amalgamation cycle; (2) adsorbed Hg in the system caused by the employment of tygon

tubing in the valving assembly; (3) the large internal diameter of the tubing contributing to the spreading of the sample plug; and (4) inefficiency of heating of the gold trap, resulting in less than 100% release of adsorbed Hg from the amalgamator.

(A) CHANGES TO INTERNAL HARDWARE OF GALAHAD/MERLIN.

A series of initial changes were performed to the system in an attempt to improve on the reproducibility and decrease the blank signal. Table 3 lists the series of primary changes to the system. The diameter of the quartz tube surrounding the gold trap in the Galahad was decreased from O.D. 8mm, I.D. 5mm to O.D. 6mm, I.D. 4mm. It was believed that the efficiency of heating of the gold trap would be improved with a decrease in both the surface area of glass and wall thickness through which the heat had to pass. The diameter of the internal tubing of the Galahad and the Merlin was decreased from O.D. 8.0 mm, I.D. 5.0 mm, to O.D. 3.2 mm, I.D. 1.6 mm and the tubing was changed from tygon to teflon. From FIA principles, miniaturization of a flow system offers the advantages of reagent economy, increased sensitivity and greater efficiency of the instrument. The internal tubing was changed from tygon to teflon because teflon is more inert and less likely to adsorb Hg^0, thereby eliminating possible signal fluctuations due to adsorption or leakage from the system. This is also why the tygon tubing surrounding the quartz tube of the Galahad, connecting it to the internal tubing of the valving system was replaced with leakproof teflon connectors.

Table 3: First Series of Changes to Galahad/Merlin System.

Area of Modification	Original	Modified
Quartz tube of Galahad surrounding gold trap	O.D. 8.0 mm, I.D. 5.0 mm	O.D. 6 mm, I.D. 4 mm
Internal tubing of Galahad and Merlin	O.D. 8.0 mm, I.D. 5.0 mm tygon	O.D. 3.2 mm, I.D. 1.6 mm teflon
Tubing connecting quartz tube of Galahad to internal valving system	tygon tubing fitted over the ends of the tube	leakproof teflon connectors with gland nuts
Gold mesh of Galahad	0.2 g	0.05 g
Connection of Sample line from Gas/Liquid separator to waste.	No connection resulted in backpressure for Hg in water studies.	Connection to waste line provides alternate flow during Vaporize and Flush periods.

It was believed that there was possible leakage of mercury vapour through the tygon tubing. Figures 34 (A) and (B) reveal the original and modified fittings over the quartz tube.

Figure 34 : Original (A) and modified (B) connections of quartz tube to internal tubing of Galahad.

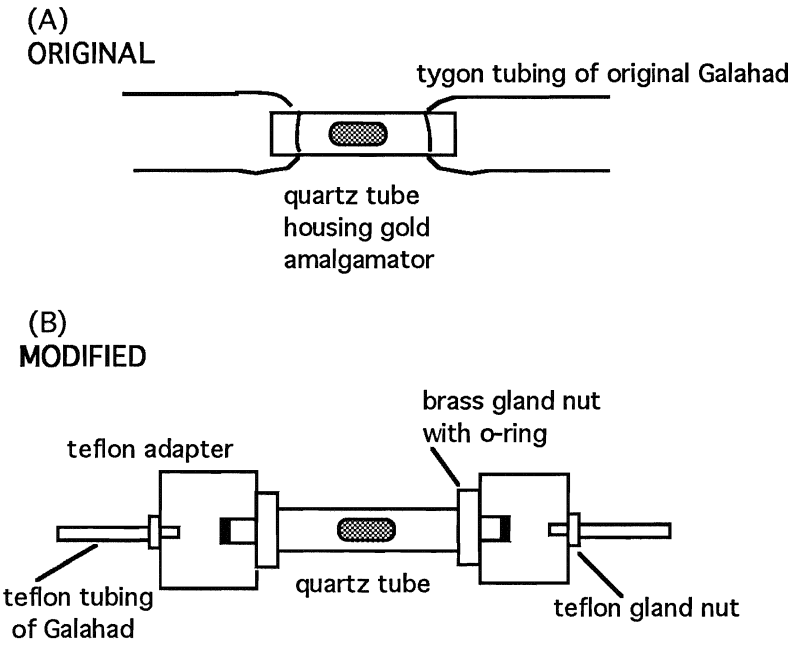

The gold mesh was decreased to 1/4 of its original size, from 0.2 g to 0.05 g. This change, in combination with the decrease of the quartz tubing surrounding the mesh, would maximize the efficiency of the heating and desorption stages of the mercury determination cycle. Examination of the internal valving connections of the Galahad revealed that the original system had no default pathway for the sample line during the Flush and Vaporize stages of the mercury determination stage. This was not a problem when mercury saturated air injections were

being performed through the septum injector but was a serious problem when the gas/liquid separator assembly was employed. When mercury solution studies were initially employed with the original system as obtained from PSA Analytical, a connection had to be made between the sample valve and the pump valve in order to avoid a backpressure problem in the gas/liquid separator. Figures 35 (A), (B), and (C) illustrate the modification to the valving system

Work on the modified system revealed that the quality of the peaks produced was improved (i.e. sharper, higher, decreased tailing), but the reproducibility was still poor and high blanks were still being produced. A carbon filter introduced between the argon tank and the system only minimally aided the problem and eliminated the possibility that the Ar carrier gas alone was contributing to the high blank signal. The focus of attention was then shifted to the valving system and flow paths of the Galahad.

Figure 35 : Illustration of addition of line from sample inlet to waste valve on original valving system of flowpath.

(A) AMALGAMATION AND COOL VALVING CONFIGURATION

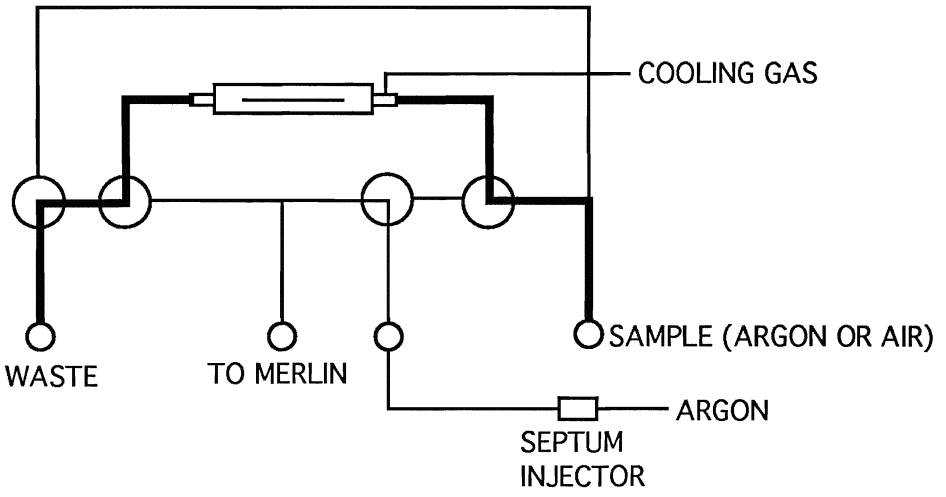

(B) Flush valving configuration

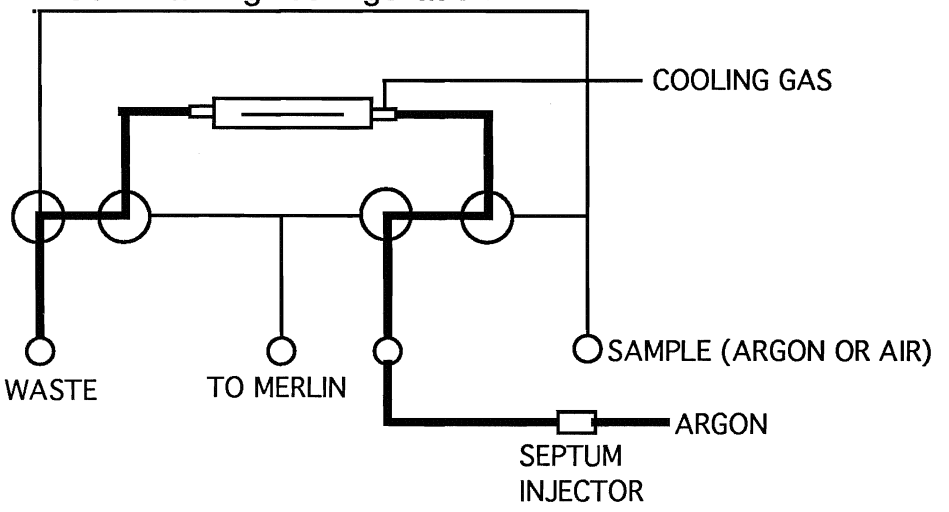

(C) Vaporize valving configuration

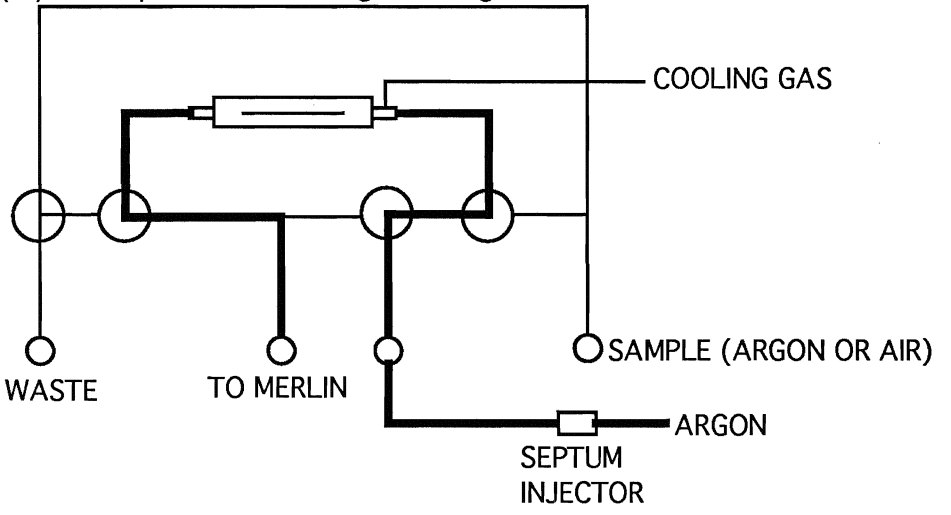

(B) CHANGES TO VALVING AND FLOW PATHS OF GALAHAD

Examination of the original valving assembly of the Galahad (figures 14 and 35) reveals that there is a relatively large distance between the sample inlet and the waste line, a potential contributor of Hg^0 to the line system. Also, the added connection between the sample inlet and waste line, described in the previous section, was not very efficient. These two valves are the most spatially separated in the system and a significant length of tubing (10-20 cm) was employed to connect them, producing a possible source of blank mercury in the line. Modifications to the valving system involved the repositioning of the valves in such a way as to maximize the efficiency of the system and minimize unwanted Hg^0 in the line. Figures 36 (A), (B), and (C) illustrate the modified flow paths of the system. The sample and waste valves were positioned adjacent to each other, minimizing their physical distance and providing a default pathway for carrier gas from the separator.

Work with the system after this series of modifications demonstrated little improvement of the blank problem with respect to mercury in solution work. Mercury in air determinations could be stabilized (figure 37) with numerous repeated cyclings of the system but this was of little consolation as the main focus of the study was on determination of Hg in water. A major component was being

Figure 36 : Modified valving system of Galahad: A, amalgamation and cool valve configurations; B, modified flush valve configuration; and C, modified vaporization valving configuration.

(A) MODIFIED AMALGAMATION AND COOL CONFIGURATION

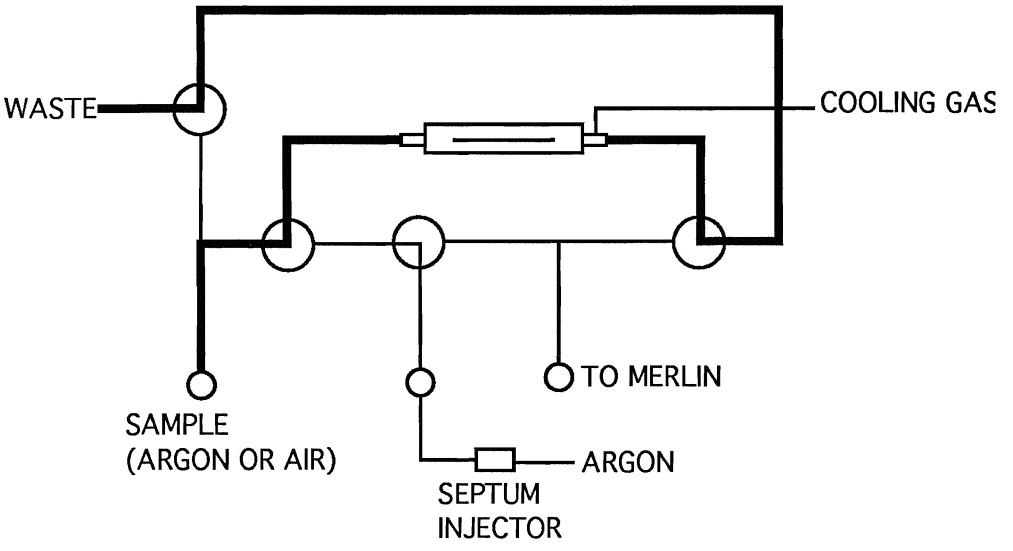

(B) MODIFIED FLUSH VALVE CONFIGURATION

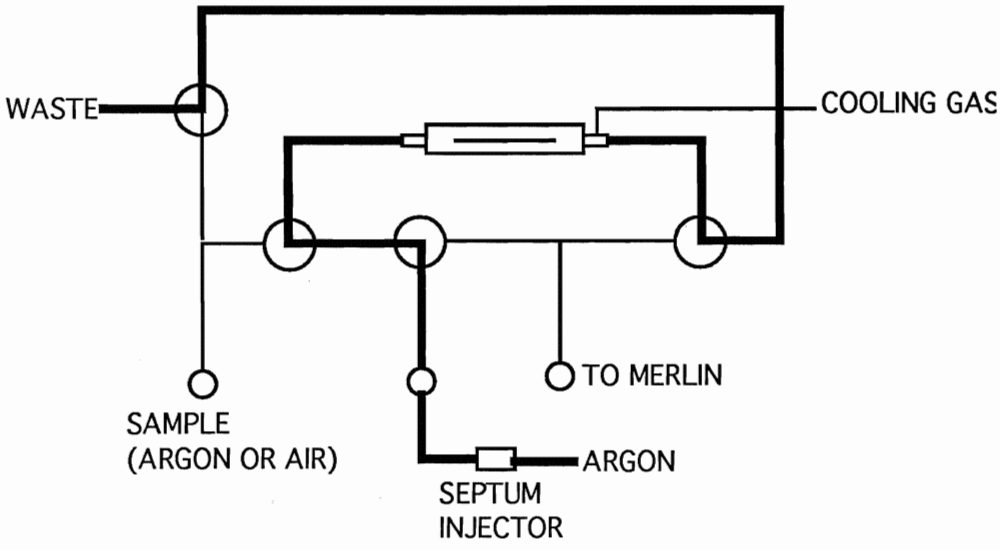

(C) MODIFIED VAPORIZATION VALVING CONFIGURATION

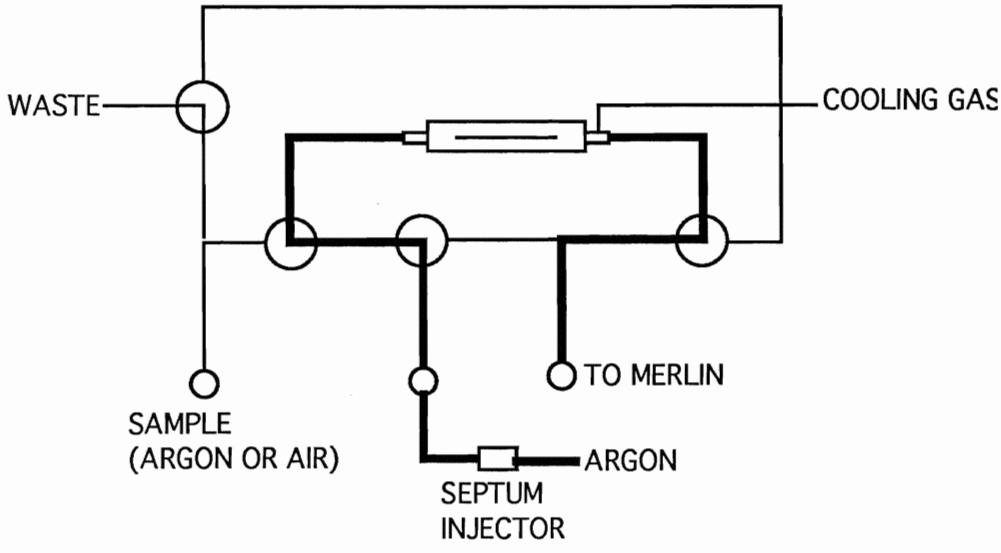

Figure 37 : Recorder output of mercury saturated air injections into the Galahad/Merlin system.

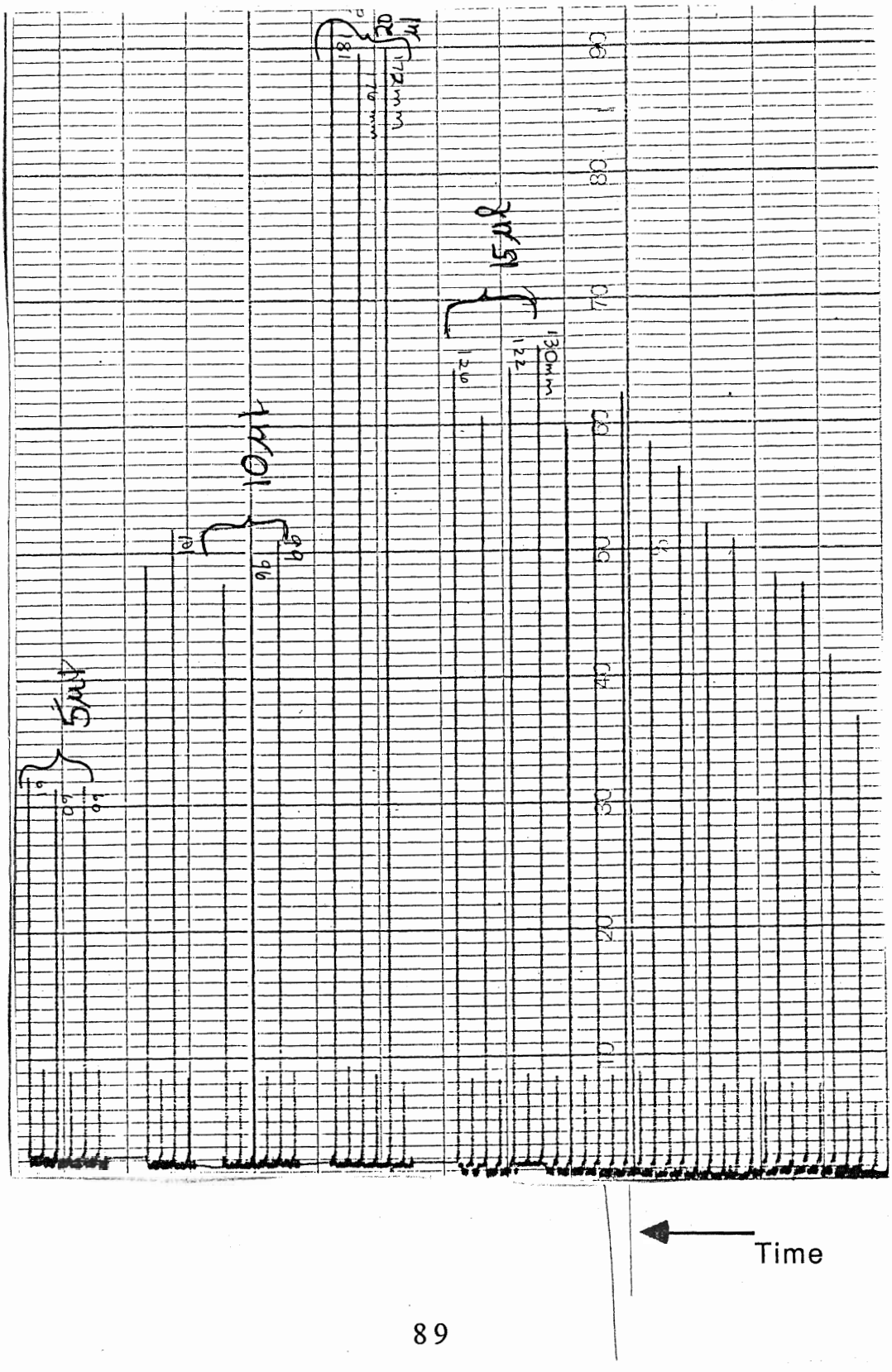

overlooked in the system that was contributing to significant blank signals and reproducibility problems.

A standard addition experiment was performed at this stage of modifications with the system to determine the concentration of mercury in the laboratory air. Air was sampled during the amalgamation stage of the system for a period of 120 s at a flow rate of 44.8 ml min^{-1}. Upon manual activation of the mercury determination stage and onset of the flush cycle, injections of mercury saturated air were made into the septum injector of the Galahad. Peak heights were obtained for 0, 5, 10, 15, 20 and 25 µl added Hg^0 saturated air at 296 K. Figure 38 illustrates the standard addition curve obtained. The ng of Hg^0 added was determined via equation 12 for each series of injections and from the x-intercept the concentration of Hg^0 in the laboratory air was determined to be 0.0014 pg μl^{-1}.

Figure 38 : Determination of mercury concentration of laboratory air via standard addition. Multiple injections of 5, 10, 15, and 20 µl of Hg saturated air (at 296 K) were performed. Intercept determined from regression equation to be -1.21 ng mercury. Mercury concentration in laboratory air determined to be 0.0135 pg µl-1.

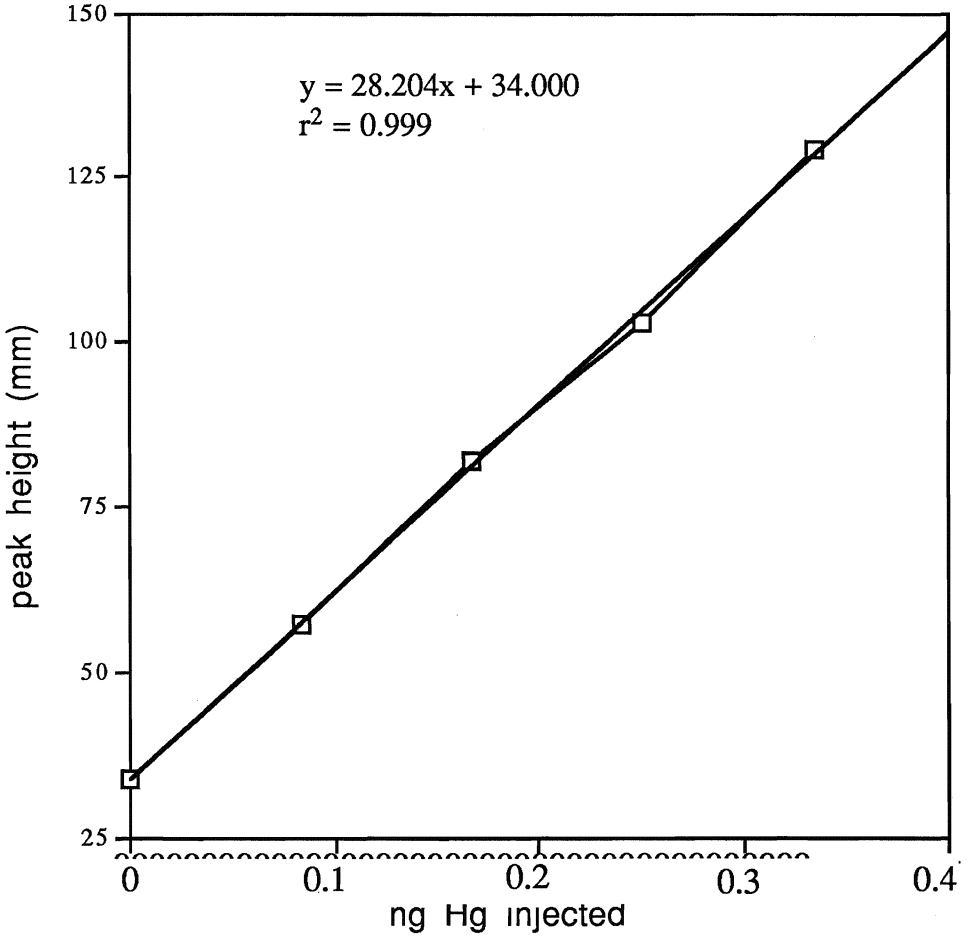

(C) COMPUTER CONTROL AND MERCURY AMALGAMATION CYCLE CHANGES.

Mercury determination in aqueous samples employing the peristaltic pump sample delivery system involved the simultaneous pumping of reagent $SnCl_2$ and carrier HCl or HNO_3 to the separator, and sample Hg^{2+} to a sample loop, the manual switching of which diverted it into the carrier stream. Upon reaching the separator, inorganic mercury is reduced by Sn^{2+} and volatile Hg^0 is stripped from solution and transported to the Galahad by argon carrier gas, passing through the frit. This sequence of events occurs during the Mercury amalgamation stage of the Galahad. Actually, it should be noted that the amalgamation stage of the Galahad is the configuration the valves maintain at all times except for the Flush and Vaporize stages of the Hg determination cycle. Thus, unless manual activation of these stages occurs, carrier Ar gas that passes through the separator passes into the line of the Galahad connecting the sample inlet to the gold trap to the waste line. It can be seen that this undesirable setup can contribute to the high blank signals, especially in situations when the instrument is turned on and left to warm up while solutions are being prepared or during pause periods when the machine is left on. Trace levels of Hg can accumulate over a few minutes and adsorb to the gold trap, resulting in high blank signals.

The quality of the gas/liquid separator also contributes to the blank problem as $SnCl_2$ and Hg^{2+} adsorb onto the frit,

contributing to a significant blank signal due to the uncontrollable release of Hg^0 into the system. Removal of the gas/liquid separator and soaking overnight produced very low blanks for the first few runs on the following day, but a steady rise in blank signal was observed following those initial ones. It became obvious that the major problems left to deal with were adsorption of unreacted reagents to the frit and the continual flow of gas from the frit through the line containing the gold trap, resulting in the steady accumulation of Hg^0 in the system that ultimately contributed to the high blank signal. These factors, along with the continual desire to automate and maximize efficiency of the system, led to the third series of changes, summarized in table 4.

The peristaltic pump, manual switching valve solution delivery setup was replaced with a sequential injection/selection valve system. With the peristaltic pump system, reagent $SnCl_2$ was continually passing through the separator, resulting in the steady adsorption and accumulation into the frit, contributing to the high blank problem. Sequential injection uses a single channel pump and solution is drawn into a holding coil by reverse rotation of the cam and is injected towards the separator by forward rotation of the cam. Rather than reagent solution continually passing through the separator, a specified volume is selected and injected, dramatically decreasing the reagent volumes required. The multiposition valve serves as a central distributor through which appropriate volumes of liquid segments are sequenced

Table 4: Third Series of Changes Implemented to Galahad/Merlin Mercury Determination System.

Area of Modification	Original	Modified
Solution delivery system	Peristaltic pump	cam driven sinusoidal flow pump
Sample injection	manual switching valve	electronically actuated multiposition valve
Hg Amalgamation	default configuration of valving system in Galahad	activation within program for specified amalgamation time
Activation of Hg Determination cycle	manual activation on front panel of Galahad	electronic activation within program
Rinsing of separator	as determined necessary by operator	automatically performed from within program
Reagent volumes employed	reagents continually pumped through system	minimal volumes of reagents injected to separator

into the holding coil and are then propelled by a flow reversal into the detector.[22]

A computer program was developed by Shaoguang Zheng[67] to control the electronically actuated selection valve and SI pump and to integrate these components with the Galahad/Merlin mercury determination system. The program controls the sample, reagent and carrier/wash solution selection and delivery to the separator, activation of the Hg Amalgamation and Determination cycles of the Galahad as well as all of the other settings associated with that instrument (ie. Flush, Vapour, Cool times), and the data acquisition, conversion and presentation features of the Merlin. Mercury determinations in solution employing the computer controlled system involved initiation of the analysis cycle within the program, upon which rinsing of the separator and pump occurs. This is followed by switching of the multiposition valve to draw carrier, sample and reagent solution into the holding coil through reverse rotation of the cam. Forward rotation of the cam propels the contents of the holding coil to the gas/liquid separator and the Hg amalgamation cycle of the Galahad is initiated. After the specified amalgamation time (selected from within the program), the Hg determination cycle of the Galahad commences and within seconds, a peak corresponding to Hg^0 concentration is displayed on the screen. Two major features of the program deal with the problems of $SnCl_2$ adsorption onto the frit and of gas from the separator continuously passing through the line containing the gold trap.

To eliminate $SnCl_2$ adsorption onto the frit, an extensive rinse cycle was incorporated into the system to rinse the separator and the lines of the valve and pump. Thus, in addition to the decrease in solution volumes being delivered to the separator as a result of sequential injection, the lines and separator are rinsed with the HNO_3 wash solution between samples.

The second modification to the system, made possible by the computer program, was the change to the Galahad Hg Amalgamation and Determination cycle. As mentioned previously, before activation of the Hg determination cycle, the valve configurations are in the default Hg Amalgamation configuration, allowing carrier Ar gas to continuously flow through the line containing the separator. A change was made that maintains the Galahad in the Flush configuration (Ar carrier gas from the separator passing directly to the waste line as in the Hg Determination valve configuration) during all times other than the Hg Preconcentration cycle, the start of which is activated by the program. Whereas previously the Hg Amalgamation valve configuration was the default, it is now activated by the program and gas flow from the separator passes through the gold trap during this period only. At all other times it is diverted to waste, eliminating the possibility of unwanted Hg^0 amalgamating onto the trap. Thus the line connecting the sample inlet, gold trap and detector is isolated from non-sample sources of Hg^0.

Injections of sample solutions into this system demonstrated a dramatic decrease in the blank signal and a

greatly improved reproducibility for repetitive injections. The program has a feature that allows for simplex optimization of as many as nine parameters. Work is currently ongoing on the optimization of parameters such as reagent volumes, gas flow rates and the Flush, Vaporize, and Cool times of the Galahad.

The detection limit of this system was determined, according to IUPAC regulations, to be 0.1 ng ml^{-1}, based on 12 blank injections. However, as the system is continually undergoing modifications, it is believed this value will change.

(D) ONGOING WORK

(1) Heating Assembly: Throughout the course of the research project with the PSA Galahad/Merlin system, there has been dissatisfaction with the heating assembly for the vaporization stage of the Mercury Determination cycle of the Galahad. It was felt that the cooling and heating of the adsorber assembly was inefficient. Resistive heating of the nichrome wire heats the wire up to 450 C but it is not known how much of that heat actually passes through the quartz tube to the gold mesh and whether a vaporize time of, say, 10 s allows for 100 % desorption of Hg^{o}. Conversely, the Cool stage of the mercury determination cycle is supposed to cool the system down to prepare for the next amalgamation cycle, and it is also unclear whether sufficient cooling of the system can occur with the present design of the heating assembly. Recently, the voltage supply to the nichrome wire heater has been increased from 22 to 32 volts, a change that has resulted

in the dramatic decrease of peak widths. This change has improved the heating efficiency of the system but the cooling problem is still present.

2. Gas/liquid Separator: The gas/liquid separator employed in this work contains a significant volume that likely contributes to peak spreading. Also, it appears that in spite of extensive rinsing of the frit, adsorption of $SnCl_2$ and $HgCl_2$ still occurs and contributes to memory effects. Investigations are currently being undertaken with alternative separator designs not containing frits. The function of the frit is to increase the surface area through which argon passes, thereby maximizing the aeration efficiency. However, in this work, the frit has also contributed unwanted memory effects and high blank signals due to the adsorption of sample and reagent.

CONCLUSIONS: MERCURY DETERMINATION

The series of changes implemented on the PSA Galahad/Merlin system obtained from PS Analytical has made it possible to detect mercury levels as low as 0.1 ng ml^{-1}. PS Analytical claims[56] that the system should easily obtain detection limits below 0.02 ng ml^{-1}, but difficulties experienced with memory effects and high blank signals make this claim difficult to support. Work with the system is ongoing with modifications of the gas/liquid separator design in hopes of eliminating the high blank signal and carryover problem which is still present.

REFERENCES

1. Skeggs, L.T., *Am. J. Clin. Path.* 1957, **28**, 311.

2. Ruzicka, J., Hansen, E.H., *Anal. Chim. Acta*,1975, **78**, 145.

3. Stewart, K., Beecher, G., Hare, P., *Anal. Biochem.*, 1976, **70**,167.

4. Ruzicka, J., Hansen, E.H., *Anal. Chim. Acta.,* 1978, **99**, 37.

5. *Flow Injection Analysis.* J. Ruzicka and E.H. Hansen, Wiley, New York, 1st edn., 1981; 2nd edn., 1988.

6. Schifreen, R.S.,Hanna, D. A., Bowers, L. D., Carr, P.W., *Anal. Chem.*, 1977, **49**, 1929.

7. Sternberg, J.C., *Adv. Chromatogr.*,1966, **2**, 206.

8. Tijssen, R., *Anal. Chim. Acta.*, 1980, **114**, 71.

9. Reijn, J. M., van der Linden, W.E., Poppe, H., *Anal. Chim. Acta,* 1980,**114**, 105.

10. Poppe, H., *Anal. Chim. Acta.*, 1980, **114**, 59.

11. Reijn, J.M., van der Linden, W.E., Poppe, H., *Anal. Chim. Acta*, 1981, **123**, 229.

12. Engelhardt, H., Klinker, R., *Fresenius Z. Anal. Chem* ., 1984, **317**, 671.

13. Ruzicka, J., Hansen, E.H., *Anal. Chim. Acta.,* 1976, **81** 387.

14. Ruzicka, J., Hansen, E.H., *Anal. Chim. Acta.,* 1977, **89**, 241.

15. Karlberg, B., Thelander, S., *Anal. Chim. Acta*, 1978, **98**, 1.

16. Baadenhuijsen, H., Seuren-Jacobs, H.E.H., *Clin. Chem.*, 1979, **25**, 443.

17. Almuiaibed, A.M., Townshend, A., *Anal. Chim. Acta.*, 1991, **245**, 115.

18. Schifreen, R.S., Hanna, D.A., Bowers, L.D., Carr, P.W., *Anal. Chem.* ,1977, **49**, 1929.

19. Pollema, C.H., Ruzicka, J., Christian, G.D., *Anal.Chem.*, 1992, **64**, 1356.

20. Ruzicka, J., Gubeli, T., *Anal. Chem.*, 1991, **63**, 1680.

21. Ruzicka, J., Marshall, G.D., Christian, G.D., *Anal. Chem.*, 1990, **62**, 1861.

22. Ivaska, A., Ruzicka, J., *Analyst*, 1993, **118**, 885.

23. Carpentier, P., *Bull. soc. ing. civ. France* ,1870, 235.

24. Volhard, J., *Prakt. Chem.*, 1874, **117**, 217.

25. Lundbak, A., *Kem. Mannedsblad* , 1943, **24**, 138.

26. McKittrich, D.S., Schmidt, C.L.A., *Arch. Biochem.*, 1945, **6**, 273.

27. Dubsky, J.V., Trtilek, J., *Mikrochemie*, 1933, **12**, 315-20.

28. Utsumi, S., *J. Chem. Soc. Jpn., Pure Chem. Sect.,* 1952, **73**, 835.

29. Iwasaki, I., Utsumi, S., and Ozawa, T., *Bull. Chem. Soc. Japan.* 1952, **25**, 226.

30. Standard Methods for the Examination of Water and Wastewater 16th Ed. American Public Health Association. American Waterworks Association and Water Purification Control Federation, Washington, D.C., 1985, pp. 286-294.

31. Methods for Chemical Analysis of Water and Wastes U.S. EPA, Cincinnati, Ohio, 1979, pp.325.1-1-325.1-3 and 325.2-1-325.2-3.

32. Analytical Methods Manual, Environment Canada, Inland Waters Directorate, Inland Waters Branch, Ottawa, NAQUADAT No. 17206 Chloride, 1979.

33. ASTM Power Plant Water Analysis Manual, American Society for Testing and Materials. Philadelphia, PA, 1984.

34. Skeggs, L.T., and Hochstrasser, H., *Clin. Chem.*, 1964, **10**, 918.

35. Technicon Instruments Corporation, Tarrytown, N.Y. Technicon method SE4-0005 FD4, 1974.

36. Ruzicka, J., Stewart, J.W.B., and Zagatto, E.A., *Anal. Chim. Acta.* 1976, **81**, 387-396.

37. Yoshinaga, T., and Ohta, K., *Analytical Sciences*, 1990, **6**, 57.

38. Basson, W.D., and van Staden, J.F., *Water Research.* 1981, **15**, 333-335.

39. van Staden, J.F., *Fresenius Z. Anal. Chem.*, 1985, **322**, 36-41.

40. van Staden, J.F., *Talanta*, 1991, **38**, 1033-1039.

41. van Staden, J.F., *Anal. Chim. Acta.*, 1992, **261**, 453-459.

42. van Staden, J.F., *Fresenius J. Anal. Chem.*, 1993, **346**, 723-727.

43. Tyson, J.F., Fogg, A.G., and Wang, X., *Quimica Analytica*, 1989, **8**, 179-189.

44. Zall, D. M., Fisher, D., and Garner, M. Q., *Anal. Chem.*, 1956, **28**, 1665.

45. *Stability Constants*, eds. Sillen, L.G. and Martell, A.E. , The Chemical Society, London, 1964.

46. Florence, T. M., and Farrar, Y. J., *Anal. Chim. Acta,* 1971, **54**, 373.

47. *Metal Toxicity in Mammals-2*, Venugopal, B., Luckey, T.D., 1978, Plenum Press, New York.

48. *Mercury Contamination: A Human Tragedy.* D'Itri, P., D'Itri, F., 1977, John Wiley and Sons, New York.

49. Hatch, W.R., Ott, W.L., *Anal. Chem.,* 1968, **40**, 2085.

50. Siemer, D., Hageman, L., *Anal. Chem.*, 1980, **52**, 105.

51. Gilbert, T.R., Hume, D.N., *Anal.Chim. Acta.*, 1973, **65**, 461.

52. Stainton, M.P., *Anal. Chem.*, 1971, **43**, 625.

53. Hawley, J.E., Ingle, J.D., *Anal. Chem.,* 1975, **47**, 719..

54. Oda, C., Ingle, J., *Anal. Chem.,* 1981, **53**, 2030.

55. Thompson, K.C., Godden, R.,C., *Analyst*, 1975, **100**, 1975.

56. Stockwell, P.B., Thompson, K. C., Henson, A., Temmerman, E., and Vandecasteele, C., *Int. Labmate*, 1989, **14**, 45.

57. Corns, W.T., Ebdon, L.C., Hill, S.J., Stockwell, P.B., *Analyst.*, 1992, **117**, 717.

58. Dumarey, R., Temmerman, E., Dams, R., Hoste, J., *Anal. Chim. Acta,* 1985, **170**, 337.

59. Anderson, D.A., Evans, J.H., Murphy, J.J., White, W.W., *Anal. Chem.*, 1971, **43**, 1511.

60. Ping, L., Dasgupta, K., *Anal. Chem.,* 1989, **61**, 1230.

61. Fitzgerald, W.F., Lyons, W.B., Hunt, C.D., *Anal. Chem.*, 1974, **46**, 1882.

62. Fitzgerald, W.F., Gill, A., *Anal. Chem.*, 1979, **51**, 1714.

63. Joensuu, O.I., *Appl. Spectrosc.*, 1971, **25**, 526.

64. Weissberg, B.G., *Econ. Geol.*, 1971, **66**, 1042.

65. *Handbook of Chemistry and Physics, 52nd Edn.*, R.C. Weast, 1971, CRC Press, Cleveland, Ohio.

66. PSA 10.511 Galahad Manual

67. S. Zheng, I.D. Brindle, unpublished results.

68. *Fundamentals of Analytical Chemistry, 4th Edn.*, Skoog, D.A., West, D.,M., 1982, CBS College Publishing, New York New York.

69. *An Introduction to Linear Regression and Correlation, 2nd Edn.*, A.L. Edwards, 1984, W.H. Freeman and Co., New York, New York.

70. D. Betteridge, *Anal. Chem.*, **50** (1978), 832A.